Abstract

Thermodynamic Investigation into the Binding Properties of Cardiac Troponin

(Human and Bovine)

By

Zachary Merle Haulsee

May 2010

Chair: Rickey Hicks, Ph.D.

Major Department: Chemistry

Troponin is an integral protein in the mechanism of muscle contraction. In order to induce cardiac muscle contraction, Ca^{2+} must bind to the TnC subunit (calcium binding subunit) of troponin to begin a conformational change in the protein. The ATPase rate of myosin with actin present is cooperatively activated by Ca^{2+} and Myosin. Ca^{2+} greatly increases the rate of ATPase activity (18-fold) and decreases the concentration of actin needed for muscle contraction activity. Ca^{2+} binding to troponin induces a conformational change that leads to a process of muscle contraction [8].

The focus of our research has been to investigate thermodynamic binding properties of various divalent metals to the Troponin C subunit of the cardiac muscle protein using isothermal

titration calorimetry. We have been able to successfully observe Ca^{2+} binding to the apo form of Bovine Cardiac TnC (BVCTnC) as well as the apo form of Human Cardiac TnC (HCTnC).

Familial Hypertrophic Cardiomyopathy, FHCM, is an autosomal dominant genetic disorder. FHCM causes an abnormal cardiac muscle contraction response in patients afflicted with the genetic mutations that result in the disorder. About 1 in 500 people, 0.2%, are afflicted with this disorder. There are many ways to approach treatment for this disease. A treatment that we have considered uses calcium sensitizing drugs. Calcium sensitizing drugs allow troponin to be more sensitive to the presence of calcium which induces cardiac muscle contraction [31].

Another focus of our research is to determine thermodynamic binding properties of calcium sensitizing drugs to troponin using isothermal titration calorimetry. Understanding the thermodynamic properties of drug-protein interaction can help reveal the mechanism of action by which the drug operates. These studies will lead to a better understanding of how calcium sensitizing drugs interact with troponin and determine their practicality in drug design for patients afflicted with familial hypertrophic cardiomyopathies.

Thermodynamic Investigation into the Binding Properties of Cardiac Troponin (Human and Bovine)

A Thesis

Presented To

the Faculty of the Department of Chemistry

East Carolina University

Greenville, NC

In Partial Fulfillment

of the Requirements for the Degree

Masters of Science in Chemistry

By

Zachary Merle Haulsee

July 2010

Thermodynamic Investigation into the Binding Properties of Cardiac Troponin (Human and Bovine)

By

Zachary Merle Haulsee

APPROVED BY:

DIRECTOR OF THESIS:_____

Anne M. Spuches, Ph.D.

COMMITTEE MEMBER:_____

Joseph M. Chalovich, Ph.D.

COMMITTEE MEMBER:_____

Andrew T. Morehead, Ph.D.

COMMITTEE MEMBER:_____

Colin S. Burns, Ph.D.

COMMITTEE MEMBER:_____

Andrew L. Sargent, Ph.D.

CHAIR OF THE DEPARTMENT OF CHEMISTRY:_____

Rickey P. Hicks, Ph.D.

DEAN OF THE GRADUATE SCHOOL:_____

Paul J. Gemperline, Ph.D.

Acknowledgements

First and foremost I would like to thank my research advisor, Anne Marie Spuches, Ph.D., for her countless hours of assistance toward my thesis and my research. Without her guidance and support I cannot imagine finishing my thesis. Her dedication to my research has been an inspiration to me. I cannot, honestly, thank Dr. Spuches enough for all of the help she has given me.

I would also like to thank Dr. Chalovich and his group at the Brody School of Medicine. Dr. Chalovich has helped me tremendously with suggestions for my research and presentations of it. His group at the School of Medicine, especially Tammy Baxley, has been able to help me with any issues I may have had purifying the protein I am studying.

Dr. Yumin Li and Dr. Shoquan Huo have helped with this collaborative project as well. Dr. Li's work in drug design and computational chemistry dealing with troponin is greatly appreciated. And, Dr. Huo's work synthesizing the drugs that Dr. Li designs has allowed me to study these drugs.

I would like to thank my thesis committee consisting of Dr. Morehead, Dr. Burns, Dr. Sargent, Dr. Chalovich, and Dr. Spuches for their help with finalizing my thesis. They all have been so gracious in lending a hand toward my research wherever it was needed.

My fellow graduate students have also helped me achieve my degree with their support and encouragement. It has been fun getting to know all of you, and I will cherish the memories of being here.

Lastly, I would like to thank my family and especially my wife, Kelin Haulsee. Kelin has stuck with me through this entire process, supporting me the entire way. My whole family's love and support has meant a great deal to me through the pursuit of my Masters degree.

Table of Contents

List of Figures

List of Tables

Abbreviations

ADP: Adenosine Diphosphate

ATP: Adenosine Triphosphate

K_D: Binding Constant

BvCTnC: Bovine Cardiac Troponin Subunit C

CTn: Cardiac Troponin

CTnC: Cardiac Troponin Subunit C

CTnI: Cardiac Troponin Subunit I

CFB: Cell Feedback Network

DMSO: Dimethyl Sulfoxide

ΔH: Enthalpy

ΔS: Entropy

EDTA: Ethylenediaminetetraacetate

FHCM: Familial Hypertrophic Cardiomyopathy

fsTnI: Fast Skeletal Troponin I

ΔG: Gibb's Free Energy

HSAB: Hard-Soft Acid-Base

HCTnC: Human Cardiac Troponin Subunit C

P_i : Inorganic Phosphate

ITC: Isothermal Titration Calorimetry

MES: 2-(N-morpholino) ethane sulfonic acid

n: Reaction Stoichiometry

STn: Skeletal Troponin

STnC: Skeletal Troponin Subunit C

ssTnI: Slow Skeletal Troponin I

Tn: Troponin

TnC: Troponin Subunit C

TnI: Troponin Subunit I

TnT: Troponin Subunit T

Chapter 1: An Introduction

1.1 An Introduction to the Anatomy of the Muscle

Muscle is the fundamental contractile tissue found in mammals and other organisms. Muscle tissue is responsible for an organism's voluntary movement and force. The tissue is also accountable for some involuntary organ function which requires the power generated from the contractile energy provided by the tissue. The power generated from the muscle tissue is an integral part of many organisms' viability in nature.

Muscle is composed of a grouping of fibers called a fascicle [1,2]. The fascicle is held together by the perimysium. The perimysium is a connective tissue that holds the muscle's bundle of fibers together [3]. Within this bundle, individual muscle fibers are enclosed by the endomysium [3]. The individual muscle fiber that is held together by the endomysium is composed of myofibrils [3]. Myofibrilis are organelles in the shape of a cylinder and are composed of the myofilaments of the muscle [1,2]. Myofilaments are the filaments of the myofibril and are made up of a thin and a thick filament [3]. The thin and thick filaments of the myofilament encompass the actomyosin proteins [3]. The various components of the muscle tissue described above are represented in **Figure 1.1**.

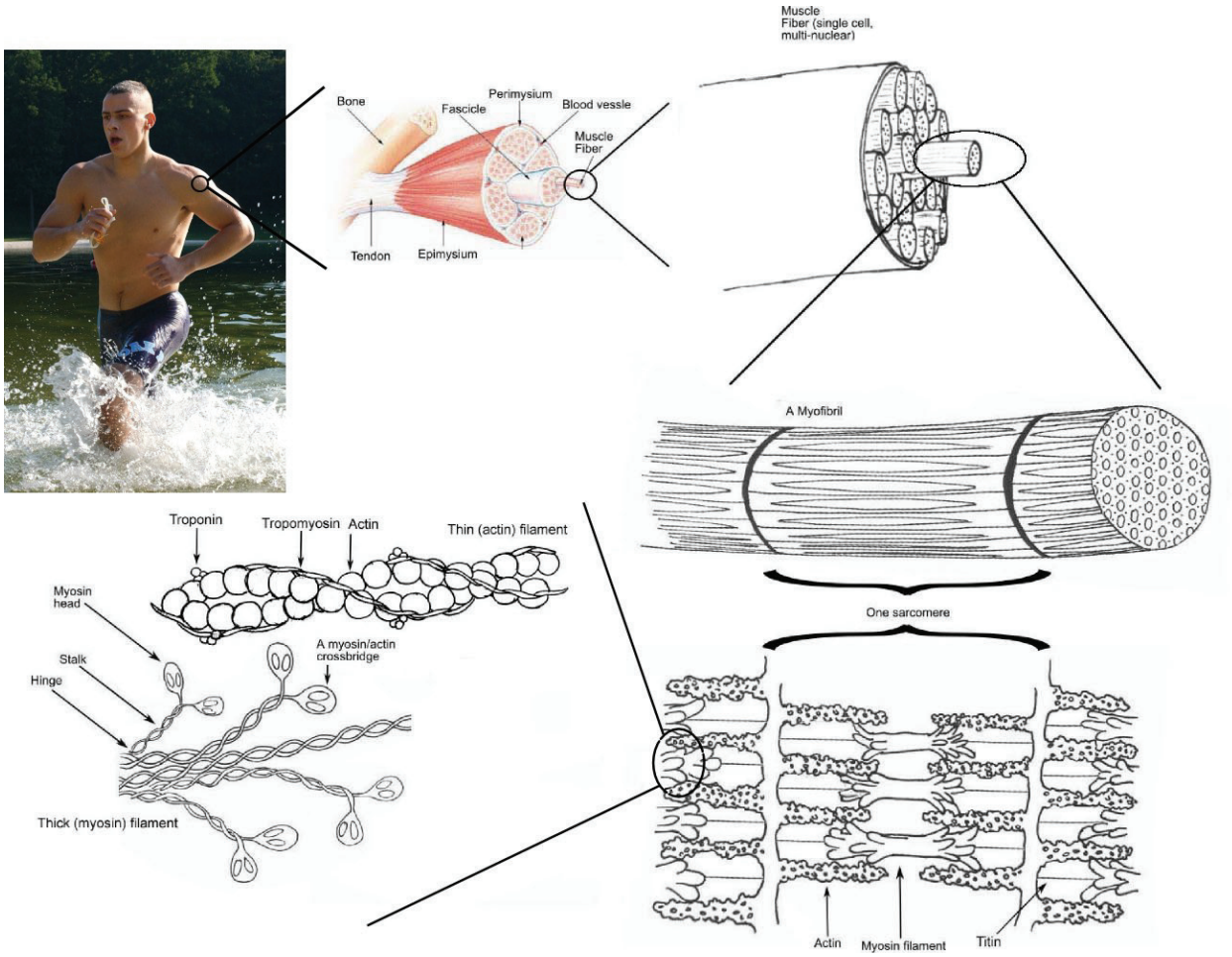

Figure 1.1: The various components of muscle as described in the previous pages [3].

The thick filament of the myofilament is composed of myosin. Myosin is a motor protein that is involved in actin derived muscle contraction and cytokinesis [4]. Myosin is a protein that has a functional gobular head and a coiled tail [4]. Myosin heads project from the thick filament of myosin toward the thin filament. The thin filament consists of the proteins actin, tropomyosin, and troponin. These three proteins interact with each other, and the thick filament,

to trigger muscle contraction. The three major components of the thin filament are depicted in **Figure 1.1**.

The myofilament can be presented as a sarcomeric representation of the filaments. The sarcomere is a basic repeating unit of the cell that is composed of the thick and thin filaments of the myofilament. Sarcomeres are the smallest contractile unit of the myofibril [3]. It is the sarcomere that gives skeletal and cardiac muscle its striated appearance [3]. The thin and thick filaments within the sarcomere interact with each other and slide along one another without changing the actual length of the filaments, themselves [3]. A representation of the thin and thick filaments in the sarcomere can be found in **Figure 1.2**.

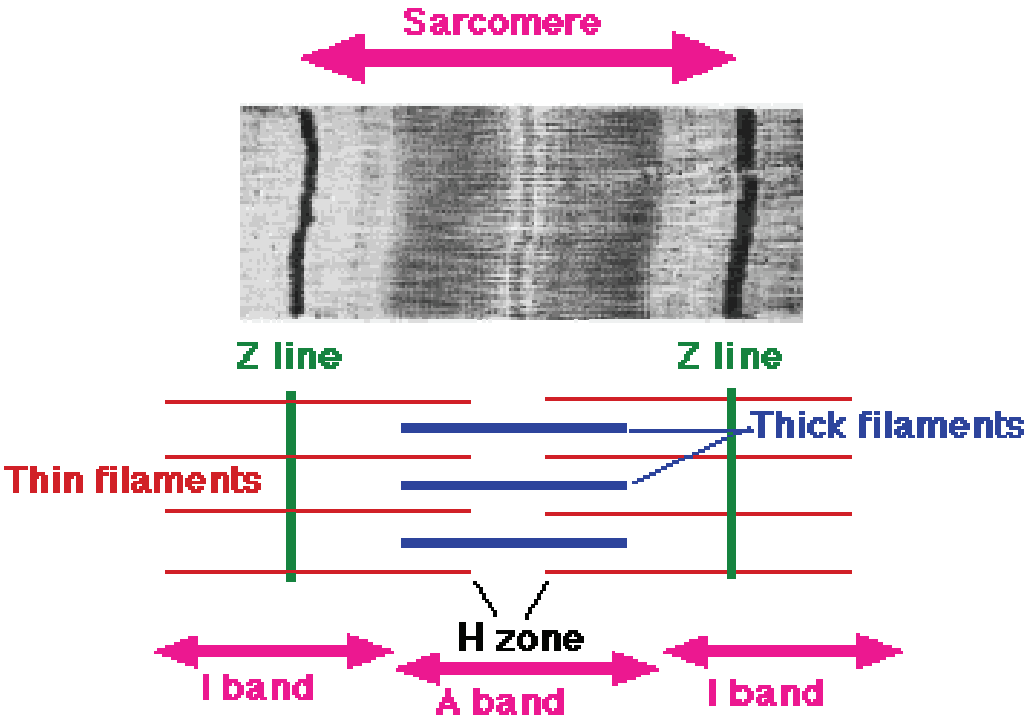

Figure 1.2. The sarcomere [5].

1.2 Mechanism of Muscle Contraction

The mechanism by which muscle contraction occurs is an intricate and interconnected progression of conformational changes, chemical binding, and protein interactions that incorporate all of the anatomy discussed in the previous section of this chapter. Muscle contraction is a process that involves multiple subunits, proteins, and divalent metal ions to proceed.

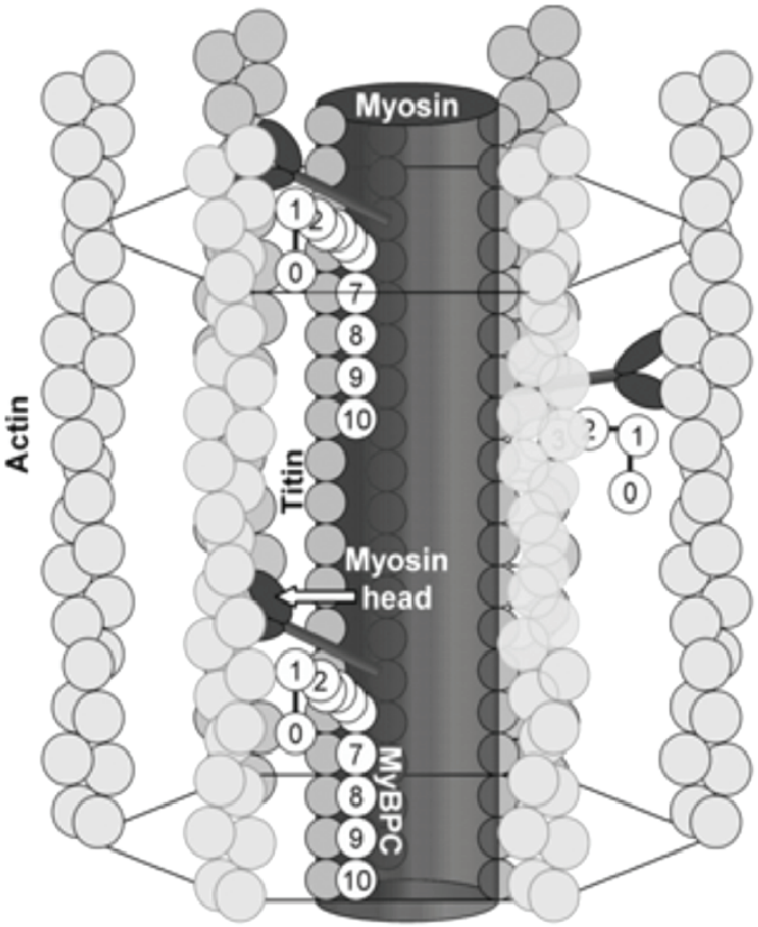

Figure 1.3: A representation of the three myosin heads projecting toward the thin filaments of actin [6].

Each equivalent thin filament, consisting of actin, tropomyosin, and troponin, has three myosin heads projecting toward it as seen in **Figure 1.3** [7]. These projections toward the thin filament are termed the myosin-actin crossbridges [7]. Cross striations of myofilaments are composed of repeating units called sarcomeres, as discussed in the previous section of this chapter [5]. Muscle contraction occurs when the thin filament slides along the thick filament causing the sarcomere to shorten [8]. Although the sarcomere, as a whole, shortens, the lengths

of the individual filaments do not get shorter, themselves [8]. **Figure 1.4** is a good illustration of the different stages of muscle contraction as it relates to the sarcomere. The thick filament of myosin is in the center of the sarcomere surrounded and intertwined with the thin filament. **Figure 1.4** displays the "A-state" as being the most relaxed position of muscle contraction. The sarcomere, in this case, is elongated and relaxed [8]. The "D-state" is the most contracted condition of the sarcomere [8]. The "D-state" is the stage in which the sarcomere is at its most diminutive point in **Figure 1.4**. The "B and C states" in **Figure 1.4** represent the intermediate steps of muscle contraction and relaxation [8]. As mentioned previously, the sarcomeric contractile mechanism is based on the notion that the actual lengths of the thick and thin filaments do not change in between the different stages of muscle contraction [8].

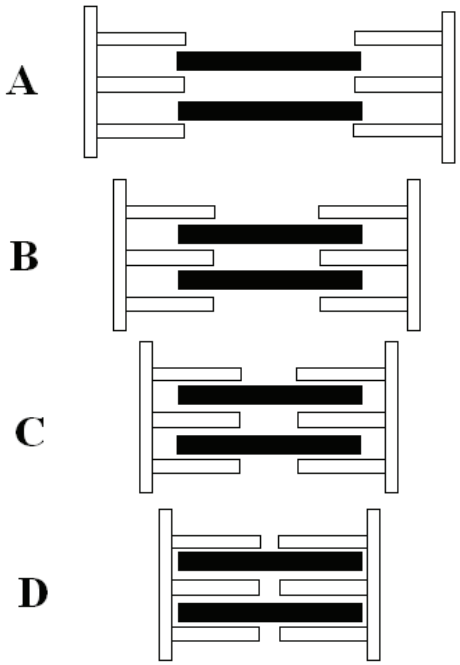

Figure 1.4: A sarcomeric observation of muscle contraction.

Muscle contraction, itself, is an ATP hydrolysis driven, cyclic interaction of myosin and actin [9]. As ATP binds close to the myosin head projections, ATP hydrolysis occurs yielding an ADP and P_i molecule [9]. Once the myosin heads bind to actin, P_i is released [9]. After P_i is released, the myosin heads propel the actin back toward the tail of the myosin, allowing actin and myosin to slide along each other [9]. Once this process is completed, the ADP is released from myosin and the head discharges from actin [9]. ATP binds once again and the process continues.

There are two ways in which muscle contraction can occur and they are not mutually exclusive interactions [10]. The first is a Ca^{2+} induced muscle contraction. The ATPase rate of myosin is cooperatively triggered by Ca^{2+} with actin present [10]. Typical ATPase activity in the absence of Ca^{2+} is slow [10]. Ca^{2+} increases the activity of the ATPase 18-fold [10]. This, in turn, decreases the amount of actin necessary for the activity to continue. The binding of Ca^{2+} to the troponin protein of the thin filament causes a conformational change which leads to muscle contraction [10].

The second way in which muscle contraction can occur is when myosin binds directly to the muscle. When myosin heads bind to actin, it augments the ATPase activity eight-fold [10]. An equivalent troponin-tropomyosin complex is known to bind seven actin monomers [10]. The two ways in which muscle contraction is induced via the microanatomical level are interconnected mechanisms of action.

1.3 An Introduction to Troponin

Before the discovery of troponin by Dr. Ebashi in 1963, muscle contraction was known to be stimulated by the presence of Ca^{2+} in the system [11]. However, the way in which Ca^{2+} interacted with the different filaments of the muscle was unidentified. Following its discovery, troponin has been investigated by many spectroscopic and structural techniques and the mechanism of action for skeletal and cardiac muscle contraction is better understood.

Troponin is broken down into three distinct subunits, all of which have their own distinct mechanism of action that eventually induces the muscle contraction response discussed previously in the chapter. The three distinct subunits are troponin subunit C, TnC, troponin subunit I, TnI, and troponin subunit T, TnT. The differing troponin subunits exist in multiple isoforms for the various types of muscle which include cardiac and skeletal muscle.

The thin filaments found in representations of the myofilament and the sarcomere are composed of actin, tropomyosin, and troponin. The troponin protein is the starting point of all fundamental chemical and micoranatomical action of muscle contraction. Troponin induces a conformational change that induces a muscle contraction response in the thin and thick filaments [12]. A ribbon structure of the entire troponin protein is portrayed in **Figure 1.5.**

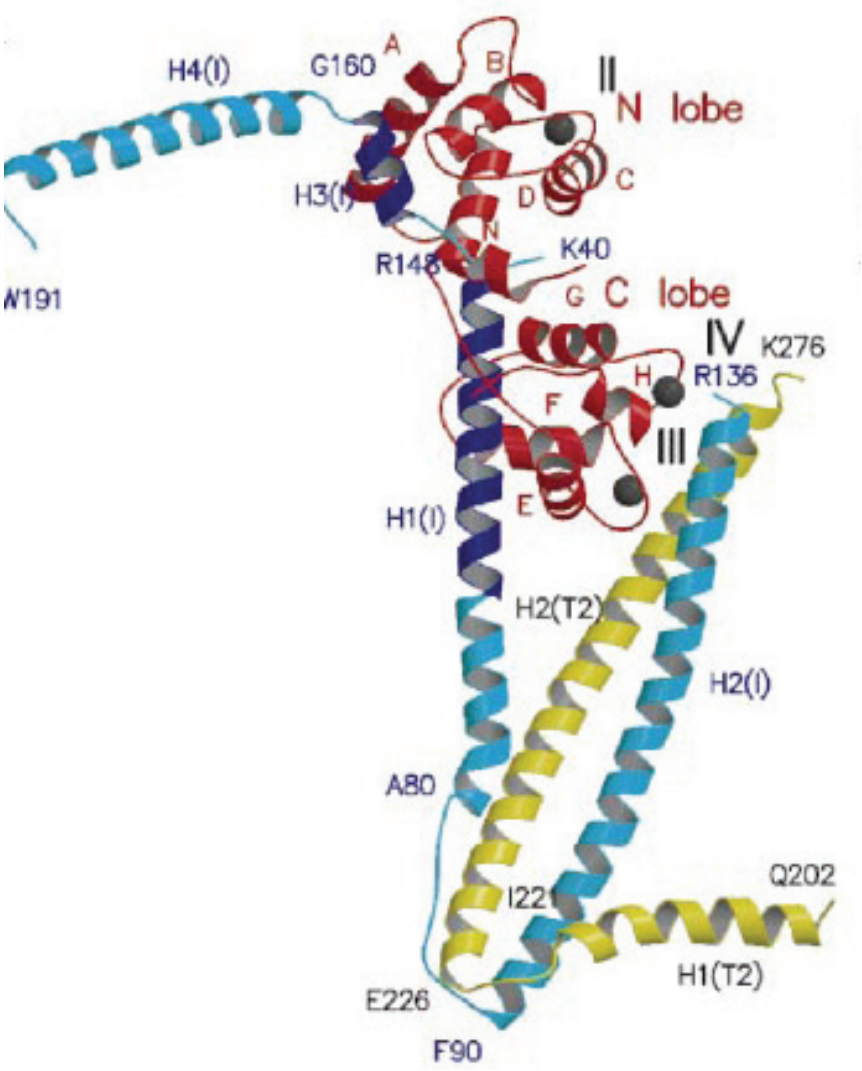

Figure 1.5: Ribbon Structure of the Entire Troponin Protein [13]. This specific ribbon diagram is the cardiac version of the protein.

A) Troponin Subunit C (TnC)

Troponin, as a whole, is an EF-hand motif protein due to the presence of its TnC subunit. EF-handed proteins are characterized by a helix-loop-helical secondary structure [14]. It is represented by the red in the ribbon diagram in **Figure 1.5.** The EF-hands typically occur in multiples of two [14]. TnC has two domains, and each domain contains two EF-hand motifs [15]. This gives TnC a total of four pairs of EF-hands. The EF-handed helices are stabilized by hydrogen bonding interactions in the loop connecting the pair of helices [15]. Although present in troponin, EF-hand motifs are found in many different types of proteins.

The first conceptual representation of an EF-hand protein was completed by Kretsinger and his research group [16]. An EF-hand protein is differentiated by an E-helix and an F-helix found in a certain formation which is conveniently located on one's own hand. The E-helix is represented by the forefinger and the F-helix is represented by the thumb as illustrated in **Figure 1.6** [17]. The calcium ion is found bound in the palm which is in between the thumb and forefinger [17]. EF-hand proteins coordinate a calcium ion with pentagonal bypyramidal coordination geometry and a coordination number of 7 [18].

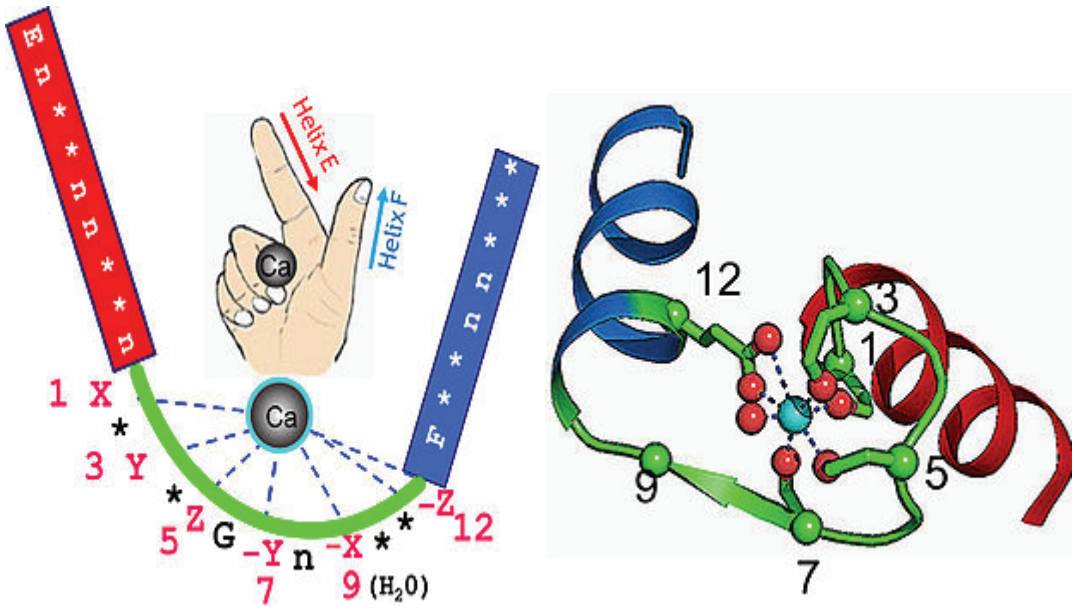

Figure 1.6: A representation of an EF-hand protein [19].

EF-handed proteins can exist as one of two classes of the protein motif. The first characterized EF-hand protein by Kretsinger fit into the class of EF-handed proteins called Ca^{2+} buffers [16]. Ca^{2+} buffers regulate the interaction between the Ca^{2+} present in the cell and other proteins in the cell [16]. This class of EF-handed proteins can either subtract the amount of Ca^{2+} available to interact with other proteins, or these Ca^{2+} buffers can distribute the effects of the Ca^{2+} present throughout the entire cell [16].

TnC fits into the other specific class of EF-handed proteins called Ca^{2+} sensors [16]. Ca^{2+} sensors allow an increasing concentration of Ca^{2+} to induce one or more signals [16]. These signals are carried by the EF-handed protein and generate biochemical responses that can result in different outcomes, including conformational changes [16].

Because Troponin subunit C (TnC) is a Ca^{2+} sensory EF-handed protein, TnC functions as the Ca^{2+} binding subunit of troponin. TnC binds calcium ions to induce a conformational change in troponin subunit I (TnI). TnC consists of two different domains, the N-domain and the C-domain, each having two EF-hands in their structure [13]. The C-domain, or structural domain, binds two calcium ions with high affinity, $K=10^7$ M^{-1} [20, 21]. Under physiological conditions, Ca^{2+} displaces Mg^{2+} from the high affinity sites [21]. Muscle contraction begins when the magnesium ion is successfully displaced from these sites. Mg^{2+} has been shown to possess a weak binding affinity, on the order of $K=10^4$ M^{-1} [21]. It is because of this weak binding affinity that calcium can readily displace magnesium from the protein's divalent metal binding sites.

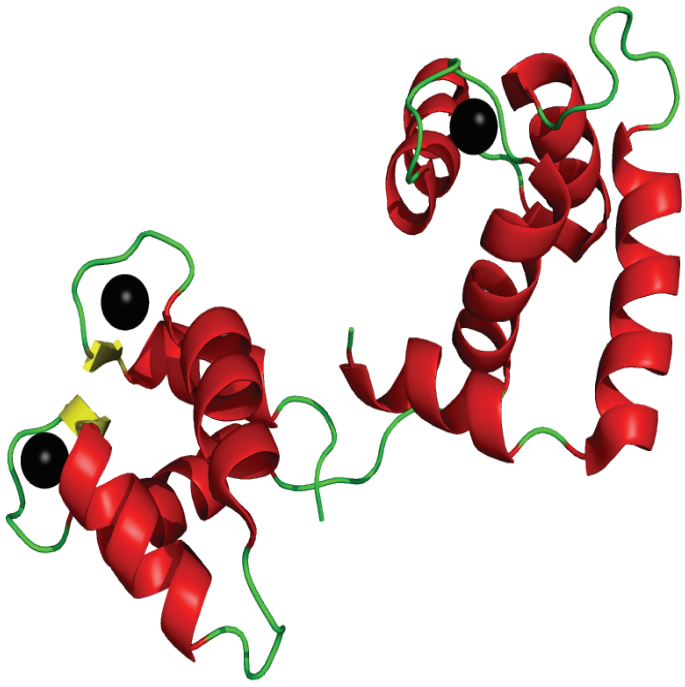

Figure 1.7: Ribbon Structure of Cardiac Troponin C (CTnC). This representation depicts the four EF-handed proteins consisting of two domains joined together by a flexible linker [22].

There are two major isoforms of TnC that exist in the human body. Skeletal TnC, or STnC, is the most prevalent form of TnC found in the body. It is found in every form of muscle tissue excluding cardiac tissue. Cardiac TnC, or CTnC, is only found in the heart muscle. There are some similarities and differences in the isoforms of the protein.

The C-domain of TnC is highly homologous in both skeletal and cardiac TnC [20]. The biggest difference between the two types of TnC is found in the N-domain, or regulatory domain, of TnC. The N-domain is called the regulatory domain because it is thought to be responsible for the regulation of muscle contraction. Both varieties of the domain bind with the same relative affinity, $K=10^5\ M^{-1}$ [21], but they differ in the number of calcium ions bound to the structure. In STnC, the regulatory domain binds two calcium ions [20]. But, in the CTnC version of the protein the N-domain of the protein binds only one calcium ion [20]. Both types of troponin C bind two calcium ions at their high-affinity binding sites. Only STnC binds two calcium ions at its low-affinity sites. In turn, CTnC binds only one calcium ion at a low-affinity site [20]. **Figure 1.7** illustrates the two domains of TnC. The domain with the two black spheres, representing calcium ions, is the structural domain. The domain with the one black sphere is the regulatory domain. The two globular domains are held together by a flexible linker [22]. The presence of only three calcium ions would indicate that **Figure 1.7** is a representation of CTnC. The binding sites of TnC can be represented as sites I, II, III, and IV, respectively (**Figure 1.5)**. CTnC binds calcium ions at sites II, III, and IV [13]. Site II is delegated as the one regulatory domain site [13]. A proper depiction of STnC would show a fourth calcium ion bound at site I [13, 20]. The reason for the differences in the number of calcium ions bound to the two distinct subunits is due to two dissimilarities in amino acid residues.

In addition, the affinities with which the regulatory domain and the structural domain bind calcium ions is dependent on whether the protein is in complex with other subunits of troponin, or if the C subunit is found by itself. It is thought that when the C subunit is in complex with the entire protein or with the troponin I subunit, that the binding affinities for Ca^{2+} increase by an entire order of magnitude [21, 23].

Two aspartic acid residues at the 29 and 31 positions of STnC account for the binding of the second calcium ion within the regulatory domain of the protein [20]. These acidic residues have negative charges at physiological pH which allow for binding to the divalent metals at this extra site. CTnC, instead, has a leucine residue and an alanine residue present at the 29 and 31 positions of the protein, repectively [20]. The substitution of acidic amino acid residues for nonpolar residues in the skeletal form of the protein allows for coordination to occur between those amino acids and the extra calcium ion bound to that form.

Dissimilarities also exist in the way in which the two isoforms of TnC mechanistically act when binding Ca^{2+} ions. STnC switches from a closed to an open conformation upon binding the two calcium ions to the regulatory domain [20]. CTnC, however, is thought to undergo minimal conformational change upon calcium binding to the N-domain of the protein [20]. The differences in conformational change between STnC and CTnC may be attributed to the differences in the residues of the protein.

B) Troponin Subunit I (TnI)

TnI is the inhibitory subunit of the troponin protein [13]. The subunit acts as an inhibitor by binding the actin-tropomyosin complex to TnC [13]. Binding the complex to the calcium binding subunit impedes the progress of muscle contraction. It is represented by the yellow in the ribbon diagram in **Figure 1.5.** Once calcium binds to TnC and induces a conformational change in the TnI subunit, TnI then binds to tropomyosin [24]. The binding of tropomyosin induces formation of the tropomyosin-troponin complex.

TnI exists in three different isoforms. Slow skeletal troponin I (ssTnI), fast skeletal troponin I (fsTnI), and cardiac troponin I (CTnI) differ in that they are encoded by different genes [25]. CTnI has an extended N-terminus, 32 amino acids in length, that has two protein kinase A phosphorylation sites which also sets it apart from the ssTnI and fsTnI isoforms of the protein [25].

The functional inhibitory area of cardiac TnI can be broken down into six regions of the subunit [22]. The N-terminal region contains an extra extension for the cardiac form of the protein [22]. The second region binds the C-domain, or structural domain, of TnC [22]. The third region binds to troponin subunit T [22]. The fourth region, or the inhibitory region, of TnI can bind actin-tropomyosin to inhibit muscle contraction, or it can bind directly to TnC to reduce muscle contraction [22]. The fifth region, or switch region, of TnI binds the regulatory domain, or N-domain, of TnC [23]. The switch region can also operate as an activator of the conformational changes brought on by the presence of calcium in the system [22]. The final region, or the C-terminal region, of TnI binds the actin-tropomyosin complex much like the inhibitory region of the protein, but it cannot bind TnC resembling the inhibitory region [22].

C) Troponin Subunit T (TnT)

TnT is the tropomyosin binding subunit of troponin [13]. It is represented by the blue in the ribbon diagram of **Figure 1.5.** It is the largest subunit of troponin. TnT binds to actin to attach and hold the tropomyosin-troponin complex to the thin filament. TnT is separated into two distinct regions. The T1 region is responsible for TnT's interaction with tropomyosin [26]. The T2 region of TnT is responsible for TnT's interaction with the TnI and TnC subunits within the troponin protein [27]. Other than the subunit's interaction with other proteins and with other subunits within troponin, troponin subunit T's role in muscle contraction is not well understood. The T1 region of the subunit has not been fully characterized.

Chapter 2: Isothermal Titration Calorimetry

2.1 An Introduction to Isothermal Titration Calorimetry

Isothermal titration calorimetry (ITC) is a wonderful instrument to use in investigating small molecule and divalent metal binding to proteins such as cardiac TnC. ITC is a bulk thermodynamic technique that measures the heat of a reaction. ITC can accurately quantify all of the thermodymanic properties including: ΔG, ΔH, ΔS, K, and n.

Binding of a small molecule to a macromolecule generates heat (exothermic event) or absorbs heat (endothermic event). When the macromolecule is saturated with the small molecule according to its equilibrium constant, K_{eq}, the heat absorbed or gained will decrease until only the background heat of dilution is observed [28]. Fitting this data to a mathematical model provides the above thermodynamic parameters.

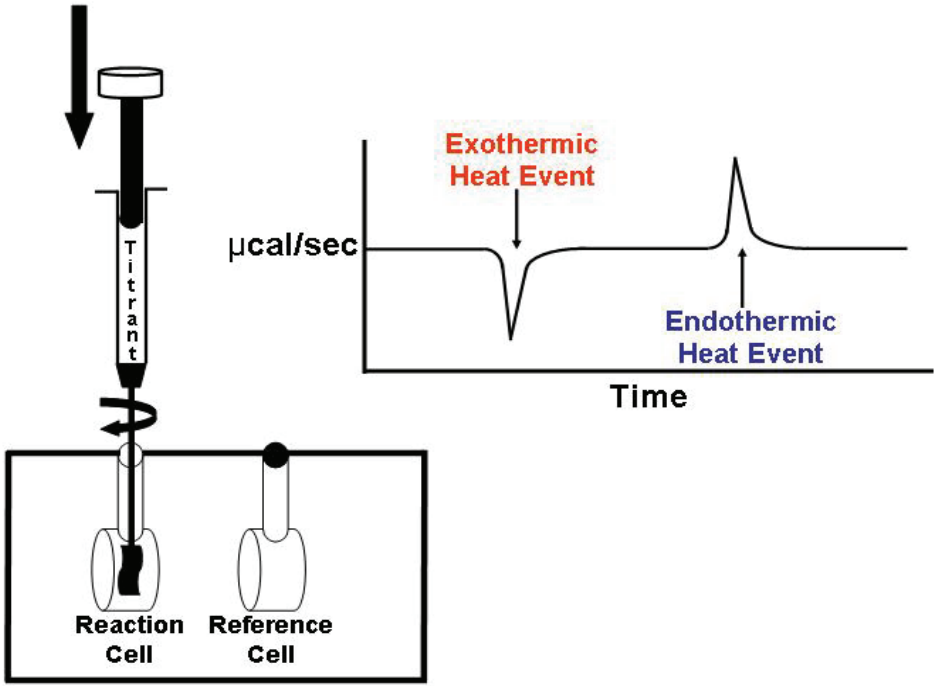

Figure 2.1 Diagram of isothermal titration calorimetry [29].

Figure 2.1 illustrates the way in which a typical isothermal titration calorimetry experiment is run. A titrant is loaded in the syringe which injects into the reaction cell under certain parameters and time intervals. The syringe is stirred at a constant speed to allow for sufficient mixing of the titrant into the analyte. A reference cell is kept at a constant temperature to compare the heat either gained or absorbed by the small molecule binding in the reaction cell. The raw data is graphed as a function of µcal/sec vs. time. If heat is lost when the titrant is injected, it will result in a negative peak corresponding to an exothermic heat event. If heat is absorbed during the injection, an endothermic heat event occurs corresponding to a positive peak in the raw data.

2.2 How Isothermal Titration Calorimetry Functions

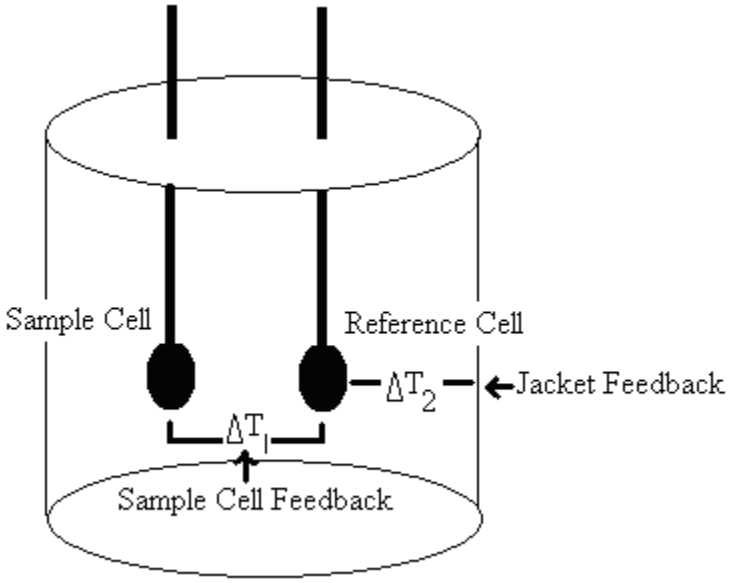

Figure 2.2 Diagram of mechanism by which isothermal titration calorimetry works.

The mechanism by which the isothermal titration calorimeter functions is an intricate procedure. A thermoelectric device is used to measure the difference in temperature between the sample cell, or reaction cell, and the reference cell [28]. This measurement is denoted as ΔT_1. A second thermoelectric device is used to measure the difference in temperature between the cells and the jacket of the isothermal titration calorimeter [28]. This measurement is termed ΔT_2. So, as small aliquots of the titrant are added into the reaction cell under the specified parameters, heat is either gained or absorbed by the sample cell. **Figure 2.2** illustrates the ITC jacket and how the instrument measures the differences in temperature.

The temperature difference between the two cells is held constant by the addition or removal of heat by a cell feedback network (CFB) [28]. It is the integral of the power required to maintain ΔT_1 constant over time that is the function of the heat being observed [28].

2.3 Thermodynamic Parameters Given by ITC

Isothermal titration calorimetry, as discussed previously, is unique in that it allows for quantification of the different thermodynamic properties of small molecule binding to a protein. A binding isotherm is obtained by injecting small aliquots of binding molecule into the analyte until saturation occurs. Each peak represents a reaction that has gone to equilibrium. The slope of an ideal isotherm reveals an accurate determination of the binding constant, or constants, K_B where M denotes the macromolecule and X denotes the ligand in the following equation [30]:

$$K_B = \frac{[MX]}{[M][X]}$$

Eq. 1

The inflection point of the binding isotherm discloses the stoichiometry, n, of the binding of the titrant with the analyte. And, the difference in the heats associated with binding and the heat associated with the heat of dilution unveils the ΔH value of the binding.

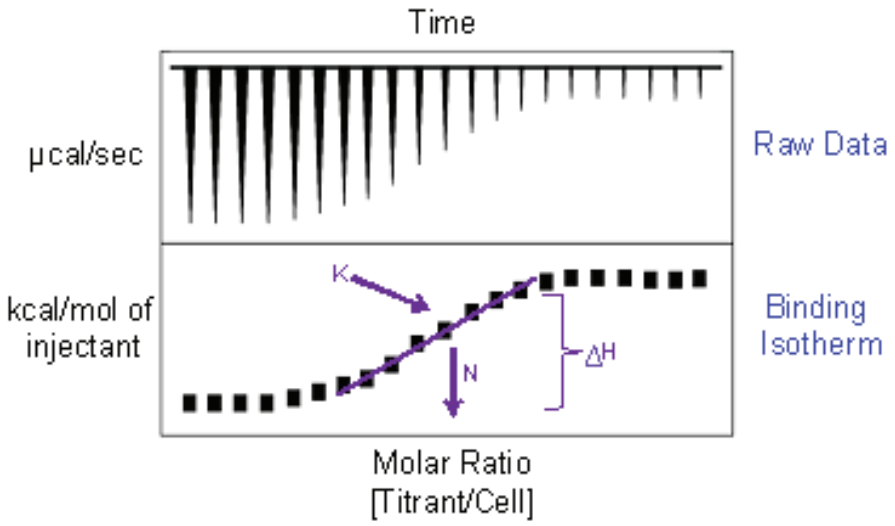

Figure 2.3 Typical ITC Raw Data vs. Binding Isotherm Graph [29].

Figure 2.3 represents a typical ITC binding isotherm with exothermic heat events. These three parameters: ΔH, K, n, unveil the totality of the thermodynamics of the binding using two fundamental equations. The Gibbs' free energy equations, found below, are the link to the other various thermodynamic parameters.

$$\Delta G=\Delta H-T\Delta S$$

Eq. 2

$$\Delta G=-RT\ln K$$

Eq. 3

Since the temperature is held constant throughout the titration, the Gibbs' free energy, or ΔG, can be determined using the binding constant found from the slope of the binding isotherm. ΔH can be determined from the difference in heats between the initial point of the binding event and the completion of the binding event associated with the titrant and macromolecule. ΔS, or the entropy, can be found once the value of the Gibbs' free energy is determined. Once one understands all of the thermodynamic contributions of the ligand binding to the macromolecule, an understanding of the mechanism and function of binding at the molecular level is better understood.

2.4 Fitting ITC Data

Fitting ITC data can be done using various computer software formats. The software that is available in the laboratory and that is most readily used is Origin™. Three common fitting models, applicable to a wide range of binding phenomena, are available within this software package. These consist of the one set of sites, two sets of sites, and sequential set of sites binding models. In general, there are six important fitting parameters to consider when fitting ITC data. These parameters include K, n, V_o, [M], [X], and Θ and are incorporated into the above mathematical models [30].

K corresponds to the binding constant which can be found by defining the slope of an ideal binding isotherm (**Figure 2.3**). The stoichiometry value, n, can also be found at the inflection point of an ideal binding isotherm and is defined by the molar ratio or ratio of [titrant] to [analyte] (**Figure 2.3**) [30]. The standard active cell volume is denoted as V_o and is unique to each brand of calorimeter. The bulk and un-complexed (free) concentrations of the macromolecule present in V_o are defined as M_t and [M], respectively [30]. The bulk and free concentrations of ligand found in V_o are defined as X_t and [X], respectively [30]. The fraction of sites on the macromolecule occupied by the ligand X is defined by Θ [30].

All fitting models evaluate the change in heat content, $\Delta Q_{(i)}$, from completion of the $i^{th} - 1$ injection to completion of the i^{th} injection for a solution contained in volume V_o [30].

$$\Delta Q_{(i)} = Q_{(i)} + \frac{dV_i}{V_o}\left[\frac{Q_{(i)} - Q_{(i-1)}}{2}\right] - Q_{(i-1)}$$

Eq.4 [30]

The second term in the above equation accounts for the displaced volume upon injection of titrant.

In general, the fitting begins with an initial guess of n single set of sites and two set of sites models, only, K, and ΔH [30]. Calculation of $\Delta Q_{(i)}$ is done for each injection and a comparison is made to the experimental value [30]. The final fit parameters are then improved using a standard Marquadt algorithm [30]. This procedure is iterated until no further improvements to the fit values occur [30] and the Chi^2 value no longer minimizes. Differences between the fitting models arise in the $\Delta Q_{(i)}$ expression derived from each binding scenario and will be discussed below.

A) One Set of Sites Model

The equilibrium expression that describes ligand binding to a single set of identical sites on a macromolecule is represented by the following equation:

$$K = \frac{\Theta}{(1-\Theta)[X]}$$

Eq. 5 [30]

Where K is the equilibrium or binding constant, [X] is the free ligand in solution, and Θ is the fraction of sites occupied by ligand X as described previously [30]. The total concentration of ligand, X_t, can be written as a function of [X] and M_t according to the following expression:

$$X_t = [X] + n\Theta M_t$$

Eq. 6 [30]

The total heat content, or Q, of the solution contained in V_o (determined relative to zero for the un-complexed species) at fractional saturation Θ is the following:

$$Q = n\Theta M_t \Delta H V_o$$

Eq. 7 [30]

Combining Eq. 5 and Eq. 6 leaves us with the following equation:

$$\Theta^2 - \Theta\left[1 + \frac{X_t}{nM_t} + \frac{1}{nKM_t}\right] + \frac{X_t}{nM_t} = 0$$

Eq. 8 [30]

Solving Eq. 8 for Θ and plugging the value into Eq. 7 provides us with the following equation for $Q_{(i)}$:

$$Q_{(i)} = \frac{nM_t\Delta HV_o}{2}\left[1 + \frac{X_t}{nM_t} + \frac{1}{nKM_t} - \sqrt{\left(1 + \frac{X_t}{nM_t} + \frac{1}{nKM_t}\right)^2 - \frac{4X_t}{nM_t}}\right]$$

Eq. 9 [30]

It is important to note that the floating variables in the above equation are n, K, and ΔH. The parameters X_t, M_t, and V_o are known values that are input prior to the fitting procedure [30].

B) Two Set of Sites Model

The two set of sites binding model is similar to the model above except for the addition of the second set of identical sites. The two sites are non-interacting and may be represented by the following expressions:

$$K_1 = \frac{\Theta_1}{(1-\Theta_1)[X]}$$

Eq. 10 [30]

$$K_2 = \frac{\Theta_2}{(1-\Theta_2)[X]}$$

Eq. 11 [30]

The fractional sites Θ_1 and Θ_2 may be solved independently from Eq. 10 and Eq. 11 and are given below [30].

$$\Theta_1 = \frac{M_t[X]K_1}{1+[X]K_1}$$

Eq. 12 [30]

$$\Theta_2 = \frac{M_t[X]K_2}{1+[X]K_2}$$

Eq. 13 [30]

As in the above example, the total concentration of ligand, X_t, can be written as a function of [X] and M_t according to the following expression:

$$X_t = [X] + M_t(n_1\Theta_1 + n_2\Theta_2)$$

Eq. 14 [30]

Substituting Θ_1 and Θ_2 into Eq. 14 provides the following expression:

$$X_t = [X] + M_t\left(\frac{n_1\Delta H_1 M_t[X]K_1}{1+[X]K_1} + \frac{n_2\Delta H_2 M_t[X]K_2}{1+[X]K_2}\right)$$

Eq. 15 [30]

The total heat content, or Q, of the solution V_o at fractional saturation Θ is the following:

$$Q_{(i)} = M_t V_o(n_1\Delta H_1\Theta_1 + n_2\Delta H_2\Theta_2)$$

Eq. 16 [30]

Substituting Θ_1 and Θ_2 into Eq. 16 gives us the final expression for $Q_{(i)}$:

$$Q_{(i)} = M_t V_o\left(\frac{n_1\Delta H_1 M_t[X]K_1}{1+[X]K_1} + \frac{n_1\Delta H_2 M_t[X]K_2}{1+[X]K_2}\right)$$

Eq. 17 [30]

It is important to note that [X] in the above equation is obtained by Newton's method from Eq. 15 [30]. Once obtained, $Q_{(i)}$ can be solved using the Marquadt least squares procedure with initial guesses made for n_1, n_2, K_1, K_2, ΔH_1, and ΔH_2 [30].

C) Sequential Binding Model

In a sequential set of sites binding model K_1, K_2, K_3,… are defined relative to the progress of the saturation [30].

$$K_1 = \frac{[MX]}{[M][X]} \qquad K_2 = \frac{[MX_2]}{[MX][X]} \qquad K_3 = \frac{[MX_3]}{[MX_2][X]}$$

Eq. 18 [30]

This means that one cannot distinguish between the sites that are saturated and that only the total number of saturated sites can be determined. The binding sites are a function of the progress of saturation. The concentrations of all complexed species [MX_i] can be expressed in terms of [M] [30]. Here we introduce a new parameter, F_i, which is the fraction of the macromolecule having i bound ligands [30]. For simplicity, we will consider only a three site system which is applicable to our studies.

$$F_o = \frac{1}{1 + K_1[X] + K_1K_2[X]^2 + K_1K_2K_3[X]^3}$$

Eq. 19 [30]

$$F_1 = \frac{K_1[X]}{1 + K_1[X] + K_1K_2[X]^2 + K_1K_2K_3[X]^3}$$

Eq. 20 [30]

$$F_2 = \frac{K_1 K_2 [X]^2}{1 + K_1[X] + K_1 K_2 [X]^2 + K_1 K_2 K_3 [X]^3}$$

Eq. 21 [30]

$$F_3 = \frac{K_1 K_2 K_3 [X]^3}{1 + K_1[X] + K_1 K_2 [X]^2 + K_1 K_2 K_3 [X]^3}$$

Eq. 22 [30]

The total concentration of ligand, X_t, can be written as a function of [X] and M_t according to the following expression:

$$X_t = [X] + M_t \sum_{i=1}^{3} iF_i$$

Eq. 23 [30]

The fitting procedure is slightly more complex than previously described models. Free ligand concentration [X] must first be obtained. This is done by the bisection numerical method from Eq. 19 through Eq. 23 [30]. Once [X] is obtained, each F_i may be solved for and $Q_{(i)}$ calculated from the equation below:

$$Q_{(i)} = M_t V_o (F_1 \Delta H_1 + F_2[\Delta H_1 + \Delta H_2] + F_3[\Delta H_1 + \Delta H_2 + \Delta H_3]$$

Eq. 24 [30]

2.5 Thermodynamics Discussion

Throughout this chapter thermodynamics have been discussed, but an understanding of what the different thermodynamic parameters truly mean has not been mentioned. The Gibbs' free energy equation, Eq. 2 and Eq. 3, reveal quite a bit of information regarding a macromolecule's interaction with the titrant of interest using ITC.

Gibbs' free energy, or ΔG, is important in understanding the favorability of a reaction. A negative ΔG value corresponds to a favorable chemical reaction. This means that work is not required for the reaction to go forward. The reaction will proceed on its own regardless of an input of work. A positive ΔG value corresponds to a non-favorable chemical reaction. Work must be applied from the surroundings to force the reaction to proceed in the forward direction. Negative Gibbs' free energy values are termed exergonic and positive Gibbs' free energy values are termed endergonic. Gibbs' free energy is a function of enthalpy, entropy, and equilibrium constant values, as defined in Eq. 2 and Eq. 3.

The binding constant, or K, value gives insight into the tightness of binding associated with the ligand to the macromolecule of interest. Positive values for lnK result in negative values toward Gibbs' free energy. So the larger K value, corresponds to the more negative ΔG value. This would indicate a tighter binding. If the binding constant is greater than 1, it will result in a favorable reaction. If the binding constant is less than 1, it will result in a non-favorable reaction.

Enthalpy, or ΔH, is a function of the heat that is resultant of the titration conducted using isothermal titration calorimetry. If heat is released upon small molecule binding to the

macromolecule, there is an exothermic heat event that occurs. Exothermic heat events result in a negative value for ΔH. If heat is absorbed from the surroundings during a titration event, there is an endothermic heat event that occurs. Endothermic heat events result in a positive value for ΔH. Enthalpy will contribute to the spontaneity of the reaction if the titration results in an exothermic heat event. Conversely, enthalpy will contribute to the non-spontaneity of a reaction if it is an endothermic heat event.

Enthalpy is a function of contributions from hydrogen bonding, van der Waals forces, electrostatic interactions, π/π interactions, and water-related specific hydrogen bonding interactions [31, 32]. Hydrogen bonding contributions toward enthalpy stem from optimal positioning of hydrogen bonding donors and acceptors [31]. This is necessary to balance the loss of enthalpy due to desolvation of the polar group [32]. A multitude of changes in bond energy occur as a result of breakage and formation of hydrogen bonds, but there must be an amount of correctly positioned hydrogen bonding that occurs to offset the desolvation enthalpies. Van der Waals attractions rely on the distance of binding interactions. If the two interacting molecules are too close, there will be repulsion. If the molecules are too far apart, the affinity will be too weak for sufficient interaction to occur [32]. Electrostatic interactions can be attributed to ionic interactions of charged species. Formation of water hydrogen bonds from a ligand to water molecules deep in the active site can result in a large contribution to enthalpy [32]. This contribution to enthalpy can offset the loss of enthalpy that occurs when water is removed from the active site [32].

Entropy, or ΔS, is a bit more complicated. A positive entropy value will contribute to the spontaneity of a chemical reaction. However, negative entropic values will contribute to the

non-spontaneity of a chemical reaction. Most learn entropy as being a function of the disorder or energy dispersal created from a reaction, but entropy can be attributed to a lot of different interactions that transpire when binding occurs. Entropy can be described as a dependence on the dispersion of energy and the distribution of energy among a large number of molecular motions [33]. Equation 25 shows how entropy is a quantity of the unidirectional flow of thermal energy since Δq is the thermal heat and T is the temperature in the equation below [33].

$$\Delta S \geq \Delta q/T$$

Eq. 25

Entropy change is best described as a measure of energy's dispersion at a specific and defined temperature [33]. It can also be defined as an energy dispersal involving molecules in microstates [33].

Entropic contributions toward binding stem from hydrophobic interactions. Hydrophobic interactions can be understood by assuming that non-polar groups tend to coalesce and minimize interaction with solvent [31]. This comes from an increase in solvent entropy from the hydrophobic groups being buried and the release of water upon binding [34]. This positive entropic event is partially offset by an ordering of the ligand in the active site [34]. This hydrophobic interaction will result in a slight endothermic heat event and large positive entropy. Entropic contributions are also characteristic of miniscule loss of conformational degrees of freedom [31].

Chapter 3: Familial Hypertrophic Cardiomyopathy and Project Importance

3.1 An Introduction to Familial Hypertrophic Cardiomyopathy

Familial hypertrophic cardiomyopathy, FHCM, is a genetic disorder characterized by an abnormal growth in the wall of the left ventricle of the heart. It causes an abnormal muscle contraction response in people afflicted with the genetic disorder. Multiple mutations found in cardiac troponin have been linked to this disease. FHCM transpires in roughly 1 out of every 500 people making it one of the most frequently occurring genetic cardiac disorders [35]. Roughly 5-10% of people afflicted with this disorder suffer fatal cardiac arrest at some point in their lifetime [36]. It is the leading cause of sudden death in young athletes [37]. One of the more infamous cases of FHCM occurred when Hank Gathers, a Loyola Marymount basketball player, collapsed on the court during a tournament game in 1990 and died shortly thereafter. It was later found that he was afflicted with this disorder after the autopsy was conducted. The mechanism of inheritance for familial hypertrophic cardiomyopathy is not completely understood. It is thought to be an autosomal dominant trait, but it has variable penetrance to the next generation [38].

Clinical studies have shown that variance of the disease's manifestation, even within the same family, is a common occurrence. Multiple symptoms are characteristic of FHCM. People afflicted with the disorder can be asymptomatic almost their entire lives, but detection usually occurs in the first few years in adolescence [39].

3.2 Bepridil and Other Calcium Sensitizing Drugs

Bepridil can be found throughout the literature as a possible treatment for familial hypertrophic cardiomyopathy. A chemical representation of Bepridil can be found in **Figure 3.1** which depicts Bepridil in complex with HCl. The HCl is present to ensure the nitrogen atoms found in the Bepridil molecule are protonated. Protonating the nitrogen atoms cause the drug to be more soluble and prevent oxidation. Bepridil has been shown to increase CTnC's affinity for binding Ca^{2+} *in vitro* [40]. Hence, Bepridil and drugs like it have been termed: "calcium sensitizers" [40]. It has also been shown to increase the activity of the actomyosin ATPase rate *in vitro* [40]. People afflicted with FHCM may be able to take this "calcium sensitizing" drug, or others like it, to increase CTnC's affinity for Ca^{2+} as well as the actomyosin ATPase activity which should induce normal, or increased muscle contraction response from the drug therapy. But, Bepridil is not currently used as a treatment for the disorder in the United States because of dangerous side effects associated with the drug therapy.

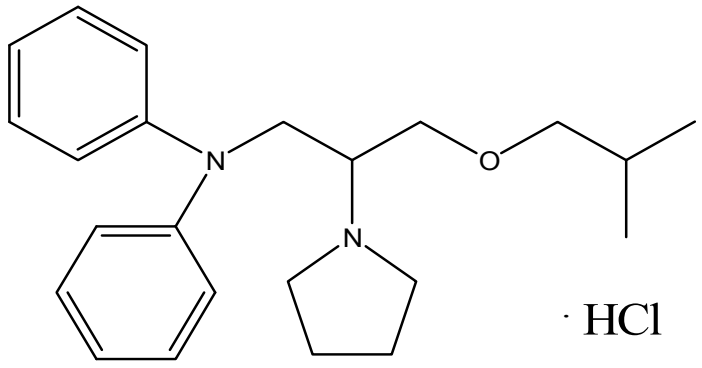

Figure 3.1 A chemical respresentation of Bepridil • HCl

There are some issues associated with Bepridil's use in the treatment of FHCM. Some of the more dangerous side effects associated with treatment using Bepridil include: acute myocardial infarction, worsened heart failure, and sudden death [41]. Some of the less dangerous, yet still problematic, side effects include: gastrointestinal problems and psychiatric issues [41]. These drastic side effects are some of the reasons that the drug is not available to people in the United States of America and why more effective yet safe treatments are necessary in the treatment of the disorder.

Even though there are definite dangerous side effects accompanied with a treatment using Bepridil, an investigation of the thermodynamics of binding to troponin subunit C may reveal a better understanding of the mechanism by which Bepridil binds to TnC. This can be essential in determining whether a treatment using other "calcium sensitizing" drugs is a viable possibility for treatment of this disorder.

Bepridil allows troponin to be more sensitive to the presence of calcium which induces cardiac muscle contraction [40]. The drug binds weakly to troponin in the absence of Ca^{2+}. Bepridil is known to bind tightly in 3 equivalents to the Ca^{2+} saturated version of the TnC subunit of troponin, when the subunit is not in complex with the rest of the troponin protein, as seen in **Figure 3.2** [40]. When the subunit is combined with the entire complex of troponin (TnI, TnT, TnC), only one equivalent of Bepridil is found to be bound to the entire protein.

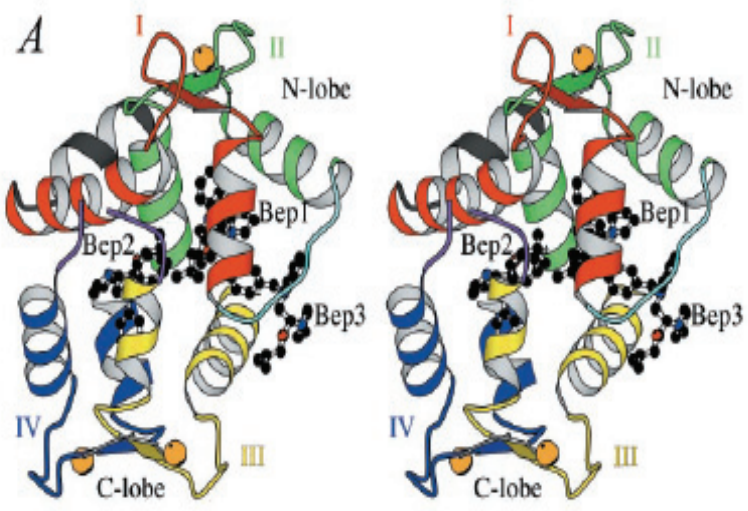

Figure 3.2 A stereo representation of 3 equivalents of Bepridil bound to a single CTnC [42].

The mechanism by which Bepridil binds to troponin has been hypothesized by the Li group, but the thermodynamic understanding of binding is still not completely characterized. The Li group has found that Bepridil stabilizes the fully open N-lobe of Cardiac TnC and a closing of the N-lobe is associated with the release of Ca^{2+} from that binding site [42]. So, Bepridil holding the N-lobe of CTnC open allows for the protein to be more sensitive to the presence of calcium. Bepridil's binding to the protein results in a rearrangement of the hydrogen bonding within the regulatory domain. Because the drug is known to bind three equivalents to the CTnC subunit, the binding of the extra two drug molecules may inhibit the binding of TnI to the subunit.

3.3 Project Importance

Considering Familial Hypertrophic Cardiomyopathy is a significant problem and affects a considerable number of the population, the way in which this disorder can be or should be treated is still debatable. We hope to uncover the possibility of using a "calcium sensitizing" drug as a treatment of this disease as opposed to other options presented in the literature.

The underlying goal of this research project is to determine thermodynamic binding properties of Bepridil to troponin using isothermal titration calorimetry. Understanding the thermodynamic properties with which a drug interacts with a protein may help reveal the mechanism of action by which the drug operates. We will be able to see how calcium sensitizing drugs interact with troponin and determine their practicality in drug design for patients afflicted with familial hypertrophic cardiomyopathies. Appreciation of the mechanism by which the drug operates is a crucial point in understanding the way in which it is best to approach treating this disease.

A basic understanding of the thermodynamic binding properties of this drug to the protein can help to explain the interactions of the drug with the protein in terms of hydrophobic interactions, electrostatic interactions, hydrogen bonding, conformational changes, and other mechanistic properties [31].

Historically, drug design began by investigating the binding constant, K_d, to determine the tightness of binding associated with the drug and the target site of action. However, drug targets with high K_d's do not necessarily equate to useful drugs. ITC has given the researcher the opportunity to look at other thermodynamic properties of the drug's interaction with a protein.

ΔG reveals the tightness of binding of the drug to the protein. A largely negative ΔG reveals a spontaneous reaction in which the drug binds tightly to the protein. When determining how this calcium sensitizing drug operates, it will be of importance to note if the reaction is entropically driven, enthalpically driven, or driven by a combination of both parameters. Enthalpy measured from the isothermal titration calorimeter reveals the strength of Bepridil's interaction with the protein. A reaction is enthalpically driven when ΔH is largely negative. This contribution toward ΔH is characteristic of van der Waals interactions, hydrogen bonding properties, electrostatics and π/π interactions [31].

Reactions that are largely entropically driven reveal a largely positive $T\Delta S$ along with a positive ΔH. Entropically driven reactions are primarily the result of hydrophobic interactions. A reaction may be characteristic of a hydrophobic interaction if ΔH is small and ΔS values are large and positive. The solvent water effect around a nonpolar solute can cause this interaction. The increase in entropy stems from the liberation of ordered water molecules around the apolar surface. It also may reflect the rigidity of the interaction of the drug with the target protein, since there will be no loss of conformational degrees of freedom upon binding to the protein. Traditional drug optimization was largely entropically driven and designed with restricted conformations to fit in a drug pocket with added hydrophobicity. This can be a problem because the drug may not work for different mutations associated with familial hypertrophic cardiomyopathies [31]. Therefore, optimizing enthalpically driven binding may be more advantageous in drug design.

3.4 Project Objectives

As mentioned previously, drugs used in the treatment of FHCM, such as Bepridil, act as calcium sensitizing agents. Prior to embarking on a thermodynamic investigation of Bepridil binding to troponin, it is important to obtain an understanding of the thermodynamics of calcium binding to the protein. Therefore, the objectives of this project are to:

- Obtain the thermodynamics of calcium and magnesium binding to bovine cardiac TnC, the calcium binding subunit of the troponin complex.
- Obtain the thermodynamics of calcium binding to the apo form of human cardiac TnC.
- Study the thermodynamics of Bepridil binding to the protein in the presence of calcium.

The C subunit of cardiac troponin, as opposed to the entire complex of the protein, was used due to the simplicity of the system. It also establishes a baseline of thermodynamic parameters for the protein.

Chapter 4: Thermodynamic Results

4.1 Sample Preparation

Thermodynamic studies involving bovine cardiac troponin C (BvCTnC) utilized protein that was previously isolated from bovine heart muscle. The protein was generously donated by Dr. Chalovich's group at the Brody School of Medicine. Later thermodynamic studies focused on the human form of cardiac troponin (HCTnC). This protein was over-expressed in bacteria cells and purified according to the following procedure obtained from the Chalovich laboratory.

An LB Agar plate containing 100 μg/mL was streaked with bacteria from a cell stock from the Chalovich group and placed in a 37°C incubator overnight to facilitate the growth of single colony cells. XL1Blue competent cells were used. A starter culture was prepared by inoculating 1 liter of sterilized LB broth containing 100 μg/mL of ampicillin with a single colony chosen from the agar plate. The starter culture was allowed to shake overnight at a temperature of 37°C and a speed of 225 rpm. The following morning, 100 mL of starter culture was dispersed into four Fernbach flasks containing LB broth and ampicillin (100 μg/L) and allowed to shake at 37°C for roughly three and a half hours. The optical density (600 nm) was taken at variable time intervals to ensure a desirable reading of roughly 1.50 A. The sample was then placed into a centrifuge and spun at 4,000 rpm for 30 minutes at 4°C. The supernatant was poured off and the cell pellet was collected. This was repeated until all of the growth had been spun down.

The next step in the growth and purification process required resuspending the cell pellet in a resuspension buffer, and lysing the cells. The resuspension buffer of 1 mM EDTA and 50

mM Tris/HCl at a pH=8.0 was used to resuspend the precipitate collected from the centrifuge into solution. Roughly 30 mL of the resuspension pellet requires 86 mg of Protease Cocktail Inhibitor, 0.4 mL of DMSO, 1.6 mL of H_2O, and 40 mg of Deoxycholate. These compounds, especially the protease cocktail inhibitor, function to preserve cellular protein composition during lysis [42]. The resulting suspension was then placed in a French Press at 2000-2500 psi to lyse the cells. This procedure was repeated, roughly 3 times, until an entirely dark and viscous liquid was retrieved from the French Press. All of this was done with ice present to prevent degrading of the sample. The French Press cell was also cooled in an ice bath before each use to ensure that the sample was maintained at a reasonably cold temperature. After lysing the cells the sample was placed in a centrifuge for 30 minutes at 18,000 rpm and 4°C. The supernatant was collected and the volume was measured. $CaCl_2$ and $MgCl_2$ were added to the sample to make its concentrations equivalent to 5 mM and 1 mM, respectively. Next, a 60% ammonium sulfate precipitation was conducted in order to clarify the protein sample and remove any cellular debris and unwanted protein. The sample was then centrifuged at 18,000 rpm for 20 minutes at 4°C, again. The supernatant was, again, collected and the final process of purification began.

A 30 mL phenyl sepharose column was set up and equilibrated with 1 M NaCl, 1 mM $CaCl_2$, and 50 mM Tris/HCl at a pH=8.0. The supernatant sample described in the previous paragraph was loaded onto the column in a controlled room temperature of 4°C and the protein was allowed to sit on the column overnight to ensure sufficient binding to the column. Two consecutive washings of the sample and the column occurred. The sample was first washed with 500 mL of 1 M NaCl, 1 mM $CaCl_2$, and 50 mM Tris/HCl at a pH=8.0. The second wash included 500 mL of 1 M NaCl, 0.2 mM $CaCl_2$, and 50 mM Tris/HCl at a pH=8.0. The washes are performed to remove impurities and to tightly bind the protein to the column to prepare for

the elution process. The protein was eluted with 400 mL of 5 mM EDTA and 20 mM Tris/HCl at a pH=8.0. The protein was collected using a fraction collector and the progress of protein elution was tested using a Bradford assay at variable intervals to check for the presence of protein. Fractions were collected at roughly 5 mL intervals using a fraction collector. The concentrations of the various fractions that tested positive using the Bradford assay were verified using a NanoDrop 2000C spectrophotometer. The concentration of the protein was calculated using an extinction coefficient of 4595 M^{-1} [44]. The samples were then tested for purity using gel electrophoresis.

Figure 4.1 shows a typical SDS-Page gel after it has been stained EZ Run Protein Gel Staining Solution from Fisher Scientific and rinsed three times with 200 mL of 18 MΩ water. The gel shows that HCTnC is present with little to no impurities present in the sample. The molecular marker to the left is a ladder that indicates increasing molecular weights as one observes from the bottom to the top of the gel. The arrows to the left of the gel denote the molecular weights that correlate with the major bands in the marker. Arrows A-G denote different fractions collected from the fraction collector during the elution process. All of the bands (A-G) fall in between the 20,040 Da. and 14,313 Da. marks. Since the bands fall in between the last band of the run and the second to last band, the bands correlate with the literature value of the molecular weight of HCTnC which is roughly 18,427 g/mol [22]. HCTnC is most prevalent in bands B through D which is why the bands in these lanes are the darkest.

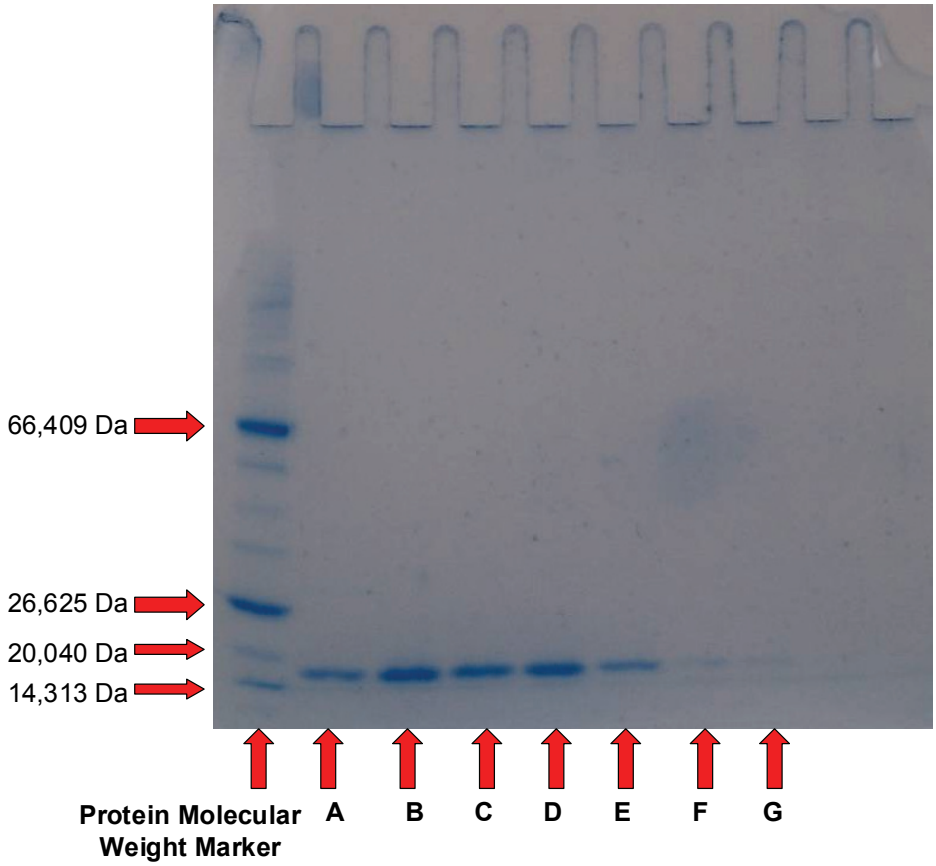

Figure 4.1. A picture of a successful gel electrophoresis using HCTnC and a molecular marker. Lanes A-G represent fractions 9-10, 11-13, 14-16, 17-19, 20-22, 23-25, and 26-28 respectively. Broad range molecular markers from Jule, Inc. were used in all gel electrophoresis.

After an electrophoresis is run and a positive result is found from the gel, we then dialyzed the protein against the standard buffer concentration of the protein, 10 mM MES, 50 mM KCl, at a pH=7.0. The dialysis was done with one liter of dialysis buffer 4 times with 2 hour spacing between the first 3, and the last dialysis was run overnight. For the Bepridil runs, a slight modification is made to the dialysis procedure. We dialyzed against 5% ethanol to ensure

compatibility with the titrant. The ethanol is present to ensure Bepridil is in solution. The dialysis of the protein sample was also done at a pH of 5.7 due to Bepridil's insolubility at a pH higher than this value. $CaCl_2$ is also present in 10 mM concentration to make sure calcium is fully bound to the protein when doing titrations involving Bepridil with the protein.

For titrations involving the apo form of the protein, Ca^{2+} must be removed from the protein to ensure decent results from the isothermal titration calorimeter. In order to remove calcium from the protein, we placed Chelex®100 into a vial containing the protein and mixed it overnight at 4°C. This allowed for ample time for removal of calcium from the high affinity and low affinity binding sites of the protein. We also ran our dialysis buffer through a Chelex®100 column to ensure removal of trace amounts of calcium.

4.2 Isothermal Titration Calorimetry Conditions

All of our isothermal titration calorimetry experiments were conducted under the same conditions, with a slight exception for Bepridil titrations, for consistency and reproducibility throughout the research and for comparisons to other studies in the literature. The buffer concentrations of all titrations were 10 mM MES and 50 mM KCl at a pH=7.0.

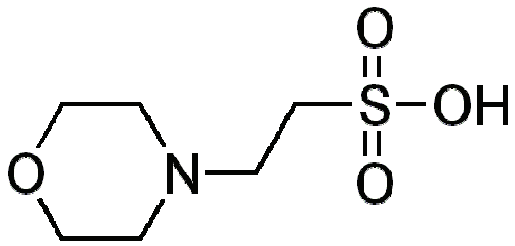

Figure 4.2. A chemical representation of MES (2-(N-morpholino) ethane sulfonic acid).

MES (2-(N-morpholino) ethane sulfonic acid) is used because it has minimal salt effects in terms of ionic strength, has little coordinating effect with metal ions, and keeps the ionic strength at a constant. Considering hard-soft acid-base (HSAB) theory, magnesium and calcium ions are hard acids and the sulfite of MES is a soft base. Since hard-hard interactions are more favorable than hard-soft interactions, the metal ions of calcium and magnesium are much more likely to coordinate with the hard base areas of the protein than with the soft base sulfonate of the MES buffer. MES buffer was also used to mimic conditions used in other studies concerning the protein. KCl is used as a buffer to mimic salt concentrations in the body.

ITC experiments were set up by delivering 8 μL injections of titrant with 250 second spacing between injections. The only exception being the initial injection point which delivers only 2 μL and only has a 120 second spacing before the second titration is delivered. The spacing between injections allows for the system to re-equilibrate and reach baseline equilibrium before performing the next injection. The calorimeter was held at a constant temperature of $25^{O}C$. Lastly, the stirring speed of the instrument was kept at 307 rpm. Stirring allows for adequate mixing of the titrant with our protein.

Titrations involving Bepridil posed a bit of a problem in regards to solubility of the "calcium sensitizing" drug. In order to get a decent concentration of Bepridil present to execute successful titrations, a pH of 5.7 is necessary and 5% ethanol must be present in the sample. Consequentially, getting Bepridil into solution requires one to first dissolve Bepridil in 100% ethanol before diluting the sample to the appropriate buffer conditions. So, buffer conditions were mimicked by adding KCl and MES buffers to ensure its consistency with the protein buffer conditions. Final buffer concentrations with Bepridil present were 50 mM KCl, 10 mM MES, 5% Ethanol, 10 mM $CaCl_2$ and a pH of 5.7. The buffer conditions for BvCTnC experiments differ slightly in terms of percentage of ethanol present. The protein was dialyzed under the same buffer conditions as described in the previous section of this chapter. The $CaCl_2$ is present so that the divalent metal is occupying all three binding sites in cardiac troponin subunit C for experiments where this is necessary.

4.3 Ca^{2+} and Mg^{2+} Binding to BvCTnC

The initial focus of our research was to investigate the thermodynamic binding properties of various divalent metals to the apo form of the Troponin C subunit of the cardiac muscle protein. Binding data and thermodynamic investigations of cardiac troponin C exist using fluorescence and microcalorimetric titration studies which serve as good comparisons to our isothermal titration calorimetry studies [21, 45-47].

The Yamada group has done extensive work investigating the thermodynamics of calcium and magnesium ions binding to the apo form of TnC [45-47]. They began their work using a modified Rhesca conduction microcalorimeter [45]. These experiments were conducted with STnC from rabbit in buffers which were different from ours: a greater concentration of KCl (100 mM), Tris-HCl (25 mM), and a greater pH = 8.83 [45]. All of these experiments were conducted at a lower temperature of 10°C. These preliminary experiments were done with $MgCl_2$ (1 mM) present [45]. The high pH was due to proton exchanges of TnC upon Ca^{2+} binding [45]. They were able to reduce this proton exchange problem to a negligible level with a high pH [45]. This paper found binding constants on the order of 10^7 M^{-1} for one high affinity binding site and 10^5 M^{-1} for the other high affinity binding site [45]. It also showed an enthalpic contribution of ΔH = -2.4 kcal/mol and an entropic contribution of $T\Delta S$ = 6.67 kcal/mol toward the one high affinity site [45]. The study also showed an enthalpic contribution of ΔH = -6.13 kcal/mol and an entropic contribution of $T\Delta S$ = .351 kcal/mol to the other high affinity site [45].

The next set of experiments by the Yamada group was done using a batch microcalorimeter [46]. These experiments were performed using BvCTnC in 0.1 M KCl, 20 mM

Pipes-NaOH and at a pH of 7.0 [46]. The experiments were conducted at varying temperatures including: 5°C, 15°C, and 25°C [46]. These experiments show lower binding affinity constants as the temperature is increased to 25°C. The binding affinity in the presence of Mg^{2+} at 25°C was $K = 10^6\ M^{-1}$ and the enthalpic contribution was $\Delta H = -4.76$ kcal/mol [46]. In both of these studies they were never able to discern the low-affinity binding site in TnC. They mentioned that if heat were generated, it was undetectably small [46].

We initiated our research with the bovine form of CTnC. This allowed us to have a reference for titrations when conducting these same experiments with the human form of the protein. As the data will show, our values confirmed a positive correlation with the literature in regards to binding constant values associated with the protein.

Most data found in this chapter is an average of multiple data sets. Throughout the chapter, one will notice that a sole example is given of raw data and a binding isotherm of interest at that point in the chapter. A data table follows each ITC raw data and binding isotherm figure which averages data from the multiple data sets. The data tables come from multiple data sets. The raw data and binding isotherm presented is a typical data set from a repeat of experiments. The other raw data and binding isotherms from which the data is compiled can be found in an appendix at the end of the thesis.

A) Ca^{2+} Binding to BvCTnC

A representative isotherm of $CaCl_2$ (0.6 mM) titrated into the apo form of BvCTnC (10 μM) is shown in **Figure 4.3**. The first heat event is highly exothermic and occurs at a molar ratio of 2 calcium ions per protein molecule. This event represents calcium ions binding to the two high affinity divalent metal ion sites in the structural domain of BvCTnC. The data may be interpreted as two calcium ions binding with the same binding constant, K, and enthalpy value, ΔH. The data may also be interpreted as two calcium ions binding with positive cooperativity where binding of the first calcium ion increases the binding affinity for the second calcium ion. In the latter model, one will not be able to separate the two sets of binding parameters since binding of the first metal will be followed by binding of the second metal with increased affinity. Therefore, the heat observed in an injection will be a summation of ΔH_1 and ΔH_2.

The second binding event occurs at a molar ratio of three and refers to the binding of the third and final Ca^{2+} to the low affinity site in the regulatory domain of BvCTnC. The data shows that the binding event is endothermic. The slopes of both the exothermic and endothermic heat events are characteristic of the binding constant, K, as described in Chapter 3 of this thesis. It is clear from the data that the first event has a sharper slope which is indicative of tightly bound calcium ions while the subsequent endothermic heat event has a gentler slope and is indicative of a more weakly bound calcium ion.

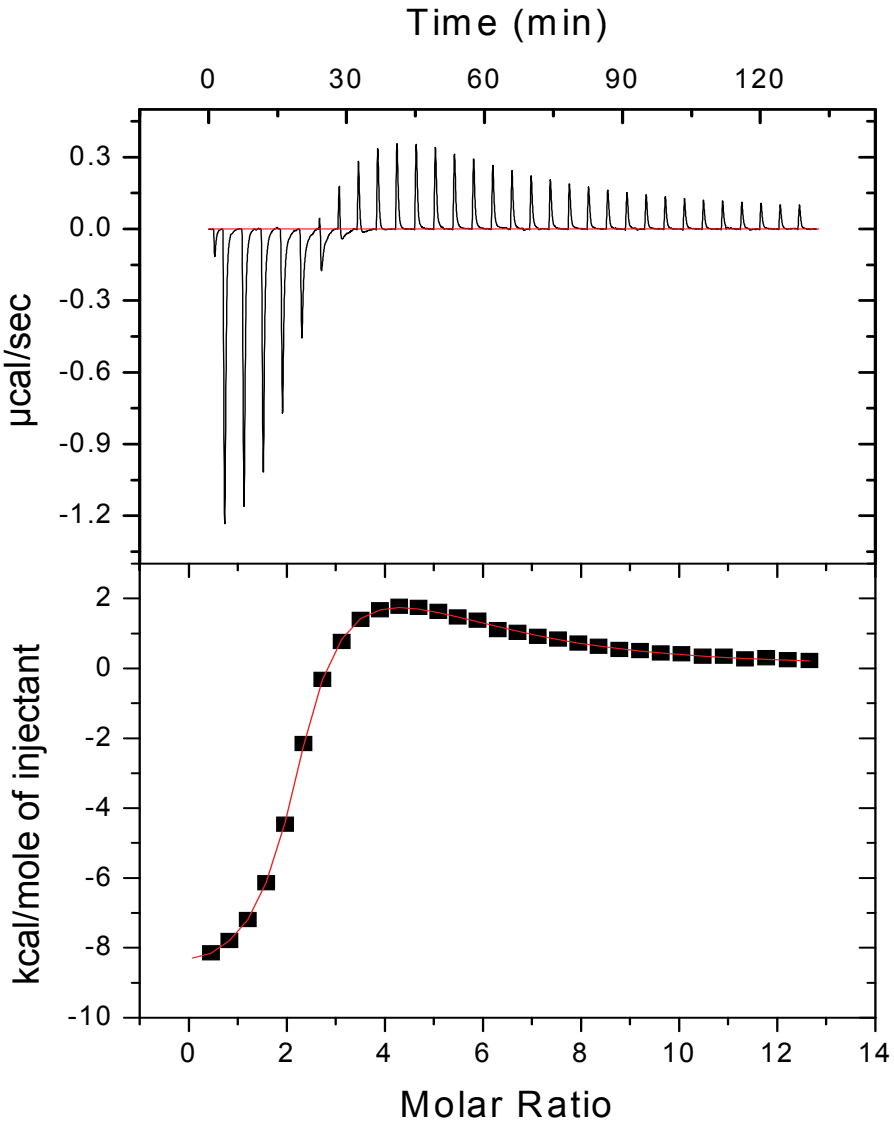

Figure 4.3. A titration of Ca^{2+} (0.6 mM) into apo BvCTnC (10 µM). Experiments were conducted at room temperature (25°C). All protein and metal solutions were in 10 mM MES and 50 mM KCl at pH=7.0 buffer conditions. Aliquots were delivered in 8 µL injections with a spacing of 250 s in between each injection. The stirring speed for the ITC was 307 rpm. This data set was fit to a "two set of sites" binding model.

I. Analysis of Fit Parameters

Two different models were used to fit the data shown in **Figure 4.3**. These included the "two set of sites" and "sequential set of sites" models and were previously discussed in chapter 3 of this thesis. In short, the "two set of sites model" considers the saturation of two independent sites within the macromolecule. Each individual site is represented by the fitting parameters n, K, and ΔH. The "sequential set of sites" model assumes a fixed sequence of binding where the first ligand always binds to site 1, the second ligand binds to site 2 and so on. The number of sites must, therefore, always be integral and are defined by the operator. The fit parameters are K_n and ΔH_n for each site where n refers to the first, second, or third ligands, etc. It is important to note that both models converge when the binding affinities of both sites differ by the several factors [30]. ITC fitting data for both models have been compiled in **Table 4.1**.

Fitting data to a "two set of identical sites" model and allowing all parameters to float resulted in values of n_1, K_1, ΔH_1, n_2, K_2, and ΔH_2 (**Table 4.1**). The n_1 value of 2.33 (± 0.03) represents the binding of two calcium ions to identical sites with K_1 and ΔH_1 values of 1.3 (± 0.1) x 10^6 and -9.31 (± 0.04) x 10^3 kcal/mol respectively. The n_2 value of 1.28 (± 0.05) indicates that only one calcium ion is bound to the second site on the protein and represents calcium binding to the lower affinity regulatory domain of BvCTnC. This site has a calcium binding affinity, K_2, of 6 (± 1) x 10^4 and ΔH_2 of 1.43 (± 0.03) x 10^4 kcal/mol. It is important to note that the binding constants obtained in the "two set of sites" model agree nicely with values reported in the literature (**Table 4.2**) [21, 45-47]. The binding constants for the higher affinity sites differ by a factor of 2, while the lower affinity binding constants agree quite closely. The differences in binding constants may stem from differing buffer conditions and issues with ionic strength. It

also may be a function of the pH that the experiment was conducted under. The Yamada group ran their experiments under higher buffer conditions. Lastly, in the Yamada paper when the temperature was increased to 25°C, the binding constant got significantly smaller [46]. The binding constants (10^6 M^{-1}) using their calorimetric methods approached our values reported in this thesis when they conducted their experiments at 25°C [46].

Table 4.1. Comparison of thermodynamic fitting parameters obtained for Ca^{2+} titrated into apo BvCTnC using the "two set of sites" and "sequential set of sites" binding models.

"Two Set of Sites" Binding Model		**"Sequential Set of Sites" Binding Model**	
High affinity binding sites representing two calcium ions.			
n_1	2.33 (± 0.03)	--	--
K_1	1.3 (± 0.1) x 10^6	$K_1=K_2$[a]	6 (± 1) x 10^5
ΔH_1	-9.31 (± 0.04) x 10^3	$\Delta H_1=\Delta H_2$[b]	-9.72 (± 0.248)
Low affinity binding site representing one calcium ion.			
n_2	1.28 (± 0.05)	--	--
K_2	6 (± 1) x 10^4	K_3	3.7 (± 0.2) x 10^4
ΔH_2	1.43 (± 0.03) x 10^4	ΔH_3	1.7 (± 0.2) x 10^4
Chi^2	1.5 x 10^4	Chi^2	1.9 x 10^4

a. Both K_1 and K_2 were constrained to equal each other during the fitting procedure.

b. Both ΔH_1 and ΔH_2 were constrained to equal each other during the fitting procedure.

Fitting the data to a "sequential set of sites" model and allowing all parameters K_1, K_2, K_3, ΔH_1, ΔH_2, and ΔH_3 to float did not yield a suitable fit because the model failed to converge on a unique set of binding parameters. It was only when K_1 and K_2, and ΔH_1 and ΔH_2 were constrained equal to each other that the curve was satisfactorily fit to the binding isotherm. Comparing K values for the high affinity binding site from both models reveals very similar affinities with the "sequential binding sites" model differing only by a factor of 2. The K values obtained for the lower affinity site also followed a similar trend differing only by a factor of 1.6. The ΔH values obtained from both models were in better agreement (**Table 4.1**).

The largest discrepancy between the two models stems from the quality of fits. The Chi^2 value for the "two set of sites" model is smaller than the Chi^2 value obtained in the "sequential set of sites" model (**Table 4.1**). As discussed in chapter 3, the Chi^2 value allows one to compare the quality of fit. A lower Chi^2 indicates a better fit to the binding isotherm and this suggests that the "two set of sits" model provides a better and more reliable fit to the data.

The poor fit of the "sequential set of sites" model is evident in **Figure 4.4**. The fit line fails to pass through the initial point in the isotherm and nearly bypasses several points in the endothermic portion of the curve. The quality of the fit generated by the "sequential set of sites" model may be due to not knowing the precise concentration of the calcium and the protein. Non-integer n values obtained in the "two set of sites" model may be an indication that the concentrations were not precise. Furthermore, the two additional fitting parameters in the "two set of sites" model may provide more variability to allow for a better fit to the isotherm. Because of the higher quality of fit obtained with the "two set of sites" model, this data will be used in later discussions.

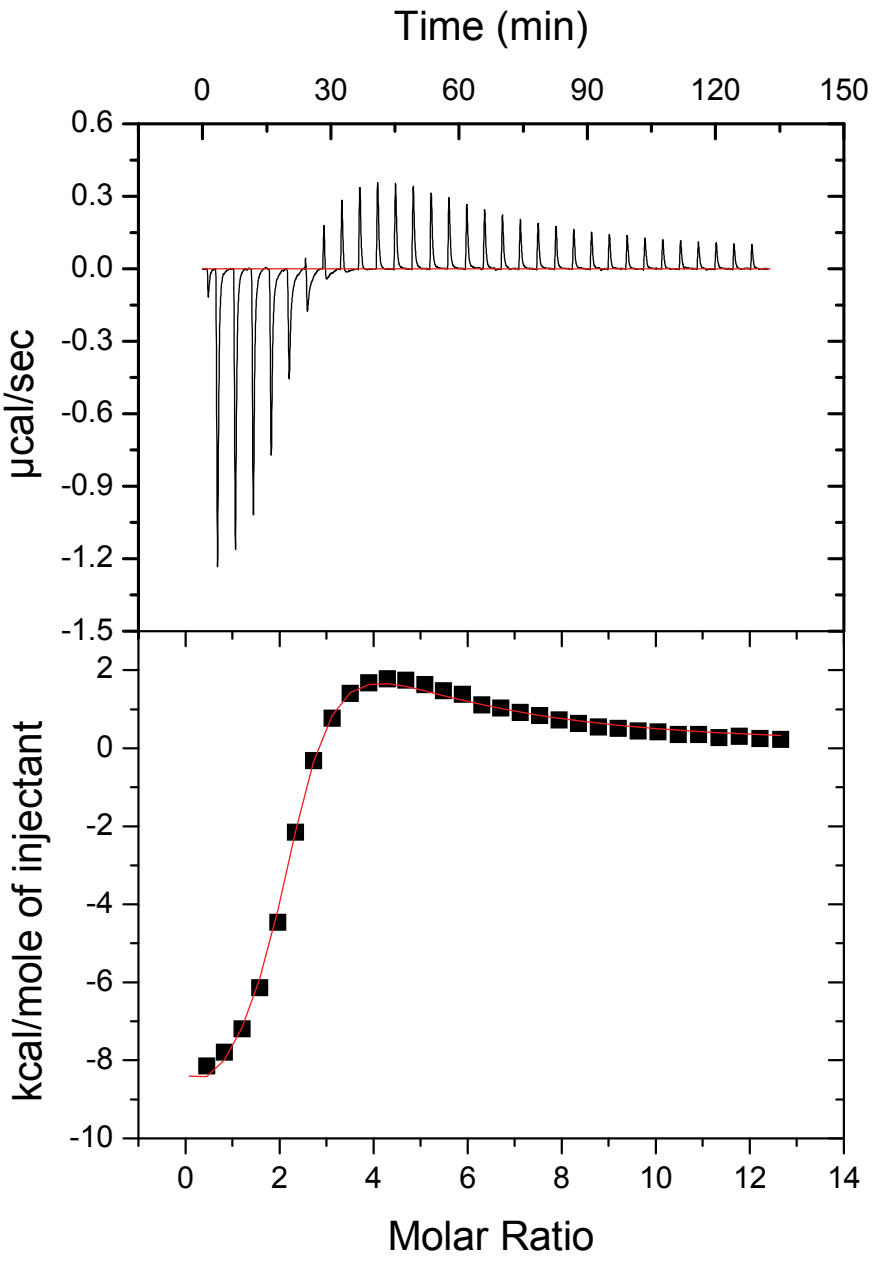

Figure 4.4. The data represents the same titration as seen in **Figure 4.3**. The data was fit to a "sequential set of sites" model.

II. Discussion of Thermodynamic Parameters

A full set of thermodynamic parameters describing calcium binding to apo BvCTnC were obtained from the "two set of sites" fit parameters and are reported in **Table 4.2**. The Gibbs' free energy of a system may be calculated from the binding constant, K, of the reaction according to the following equation:

$$\Delta G = -RT \ln K$$

Eq. 26

The entropy, ΔS, of the binding reaction may then be obtained from ΔG and ΔH according to the Gibbs' free energy equation given below:

$$\Delta G = \Delta H - T\Delta S$$

Eq. 27

Binding of calcium ions to the two high affinity sites in the protein occur with a large negative ΔG_1 (-8.3 (± 0.1) kcal/mol). Negative Gibbs' free energy values indicate favorable reactions that do not require additional input of energy to continue to completion. Binding calcium to the two high affinity sites of BvCTnC has a ΔH value of -9.31 (± 0.04) kcal/mol. Calcium binding to EDTA under similar conditions results in a ΔH value of -4.1 kcal/mol [48]. It is interesting to note that the ΔH_1 obtained in this study is roughly two times the EDTA value and represents the heat exchanged when two calcium ions bind to the protein. The entropy observed for the high affinity sites is negative as well. This corresponds to a $T\Delta S$ value of -1.0 (± 0.1) kcal/mol and is not entropically favored. The binding of calcium ions to the two high

affinity binding sites is, therefore, enthalpically driven. The –TΔS value may stem from the loss of conformational degrees of freedom of the amino acid ligands upon calcium ion binding. Furthermore, the high affinity calcium sites are required for the structural stability of the protein. This negative entropy may also be a consequence of the rigidity imposed on the protein by calcium ions binding to these two sites [40].

The second binding event represents an interesting development in regards to calcium binding to the regulatory domain of BvCTnC. The ΔG_2 value of -6.5 (± 0.1) kcal/mol indicates that the binding of calcium to the regulatory domain is still favorable. However, the reaction is not driven by the same thermodynamic parameters as previously reported for the structural domain's two high affinity sites. ΔH_2 is largely positive, 14.30 (± 0.03) kcal/mol, and enthalpically disfavored. This means that the driving force for the reaction is entropic in nature with a TΔS of 20.8 (± 0.2) kcal/mol. This is interesting because the opening of a hydrophobic area in the protein should be entropically disfavored. The entropy reported is a total contribution toward entropy, so another force must override this entropically disfavorable process. There must be some sort of conformational flexibility that is occurring that is much greater than the disfavored entropic contribution mentioned previously. ITC studies involving calmodulin, a protein of similar structure and binding characteristics, showed a similar thermodynamic profile [49].

Table 4.2. Thermodynamic Properties of Ca^{2+} Titrated into BvCTnC. This data represents a fit to a "two set of sites" binding model and is the average of two experiments.

	Average of 2 Data Sets	**Reference [21, 45-47]**
n_1	2.33 (± 0.03)	
n_2	1.28 (± 0.05)	
K_1	1.3 (± 0.1) x 10^6	1 x 10^7
K_2	6 (± 1) x 10^4	1 x 10^5
ΔG_1 (kcal/mol)	-8.3 (± 0.1)	
ΔG_2 (kcal/mol)	-6.5 (± 0.1)	
ΔH_1 (kcal/mol)	-9.31 (± 0.04)	
ΔH_2 (kcal/mol)	14.3 (± 0.03)	
$T\Delta S_1$ (kcal/mol)	-1.0 (± 0.1)	
$T\Delta S_2$ (kcal/mol)	20.8 (± 0.2)	

B) Mg^{2+} Binding to apo BvCTnC

We have also studied magnesium cations binding to the apo form of BVCTnC. *In vivo,* Mg^{2+} is known to be displaced by calcium from the three calcium binding sites of cardiac troponin C and has a binding constant of 2 x 10^4 [21]. So, an appreciation of this divalent metal's binding affinity to the apo form of the protein will be good reference to the literature as well as a good idea for how Ca^{2+} may displace the metal from the three binding sites so readily.

An isotherm representing Mg^{2+} titrated into apo BvCTnC is shown in **Figure 4.5**. The heat generated in this titration is endothermic and quite small. Although it may appear that there is a slight sigmoidal nature to the binding curve, it is difficult to differentiate this heat from the heat of dilution observed in previous titrations. The ITC data reveals that Mg^{2+} shows very weak binding, at best, and the data was not fit to any sort of binding model.

As previously mentioned, K values on the order of 10^4 have been observed for Mg^{2+} titrations into the apo form of BvCTnC [21]. Unfortunately, our data was not suitable for extracting thermodynamic values. The heat of dilution overshadows any heat associated with magnesium ions binding to the protein. A displacement reaction whereby Ca^{2+} replaces Mg^{2+} ions may yield data that will allow one to extract these parameters.

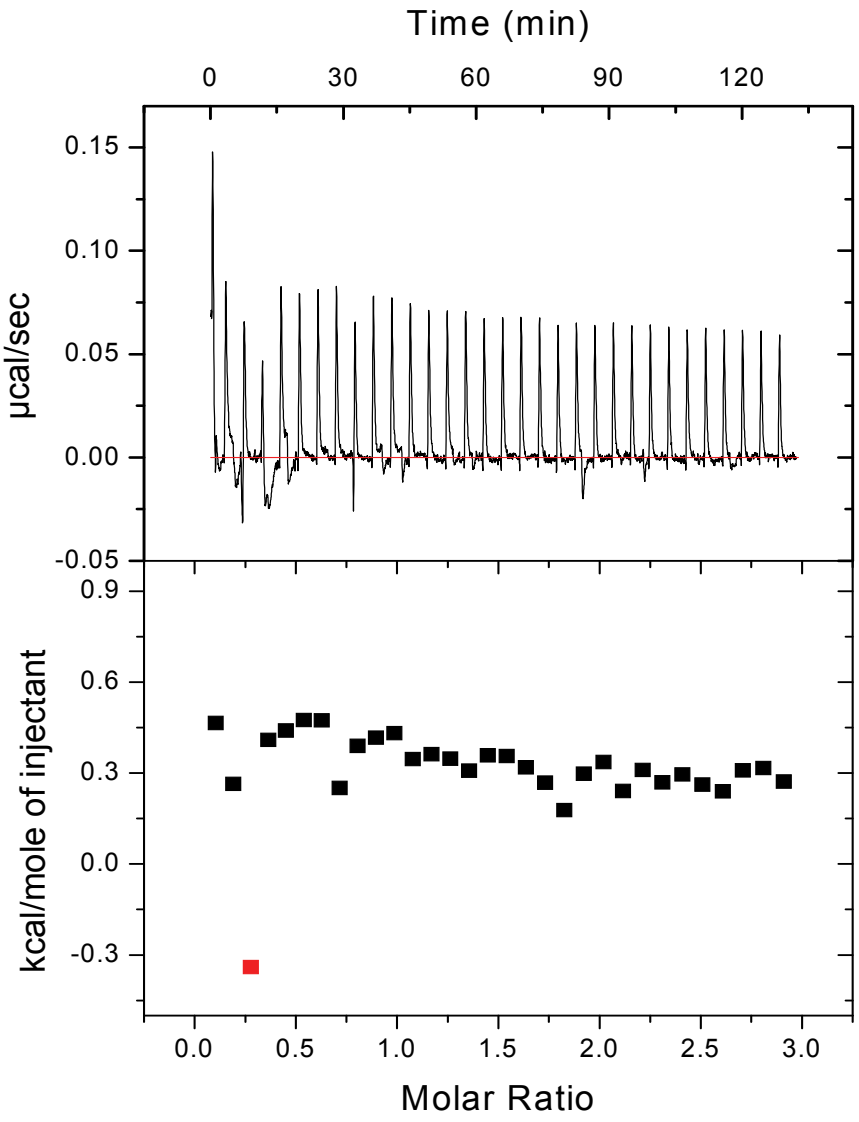

Figure 4.5. A titration of Mg^{2+} (0.6 mM) into apo BvCTnC (9 µM). The data point highlighted in red appears to be an outlier. Experiments were conducted at room temperature (25°C). All protein and metal solutions were in 10 mM MES and 50 mM KCl at pH=7.0 buffer conditions. Aliquots were delivered in 8 µL injections with a spacing of 250 s in between each injection. The stirring speed for the ITC was 307 rpm.

C) Ca^{2+} Binding to BvCTnC in the Presence of Magnesium

A displacement reaction whereby Ca^{2+} replaces Mg^{2+} ions was attempted in hopes that it would allow us to indirectly extract these parameters. A representative titration curve for Ca^{2+} ions binding to BvCTnC in the presence of Mg^{2+} (0.l mM) is shown in **Figure 4.6**. The figure shows a binding isotherm that is identical to that obtained for Ca^{2+} binding to the apo form of BvCTnC. The data in **Figure 4.6** was fit to a "two set of sites" binding model and thermodynamic values are listed in **Table 4.3**. These thermodynamic parameters are highly consistent with data for Ca^{2+} binding to the apo form of BvCTnC found in **Table 4.2**. This data demonstrates that the presence of Mg^{2+} at 0.1 mM concentrations does not interfere with Ca^{2+} binding to BvCTnC. Future studies include repeating experiments with larger concentrations of Mg^{2+} present.

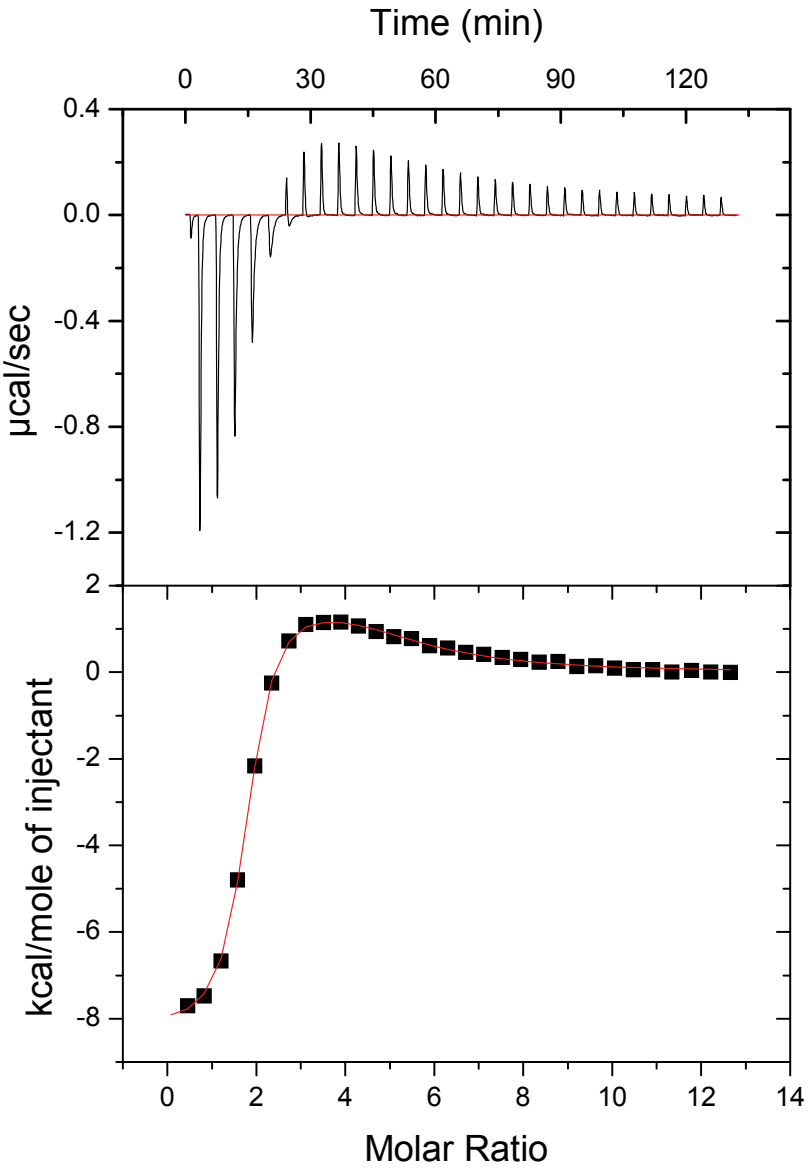

Figure 4.6. **A** titration of Ca^{2+} (0.6 mM) into BvCTnC (9 µM) in the presence of Mg^{2+} (0.1 mM). This data set is fit to a "two set of sites" binding model. Experiments were conducted at room temperature (25°C). All protein and metal solutions were in 10 mM MES and 50 mM KCl at pH=7.0 buffer conditions. Aliquots were delivered in 8 µL injections with a spacing of 250 s in between each injection. The stirring speed for the ITC was 307 rpm.

Table 4.3. Titration of calcium into BvCTnC after magnesium has been added. This data set is fit to a "two set of sites" binding model.

Thermodynamic Binding Parameters	
n_1[a]	2.03 (± 0.02)
n_2[a,b]	1.10 (± 0)
K_1[a]	1.37 (± 0.12) x 10^6
K_2[a,b]	4.50 (± 0) x 10^4
ΔG_1 (kcal/mol)	-8.37
ΔG_2 (kcal/mol)	-6.28
ΔH_1 (kcal/mol)[a]	-8.6 (± 0.2)
ΔH_2 (kcal/mol)[a]	15.3 (± 0.5)
$T\Delta S_1$ (kcal/mol)	-0.23
$T\Delta S_2$ (kcal/mol)	21.58

a. Error values were taken from Origin and reflect the error in the fit values.

b. An error of zero means that the parameter was fixed during the fitting procedure and not allowed to float

4.4 Human Cardiac TnC (HCTnC)

The human cardiac troponin C is, by far, the most interesting and valuable form of the protein. A thermodynamic investigation of divalent metal binding to the protein is essential in understanding the mechanism by which the protein binds calcium. A better appreciation of the mechanism can help drug developers develop better "calcium sensitizers."

A) Ca^{2+} Binding to HCTnC

A representative isotherm of a Ca^{2+} titration into apo HCTnC is shown in **Figure 4.7**. The binding isotherm is, in general, similar to isotherms obtained from the bovine form of the protein. Both titrations begin with an exothermic heat event (-8 kcal/mol) that transitions into an endothermic heat event during the course of the experiment. At a molar ratio of 4.5, the protein becomes saturated with calcium, and the signal observed matches the heat of dilution of calcium into buffer. The exothermic phase of both titrations correspond to the binding of 2 calcium ions to the high affinity sites of the protein, while the endothermic phase is indicative of calcium binding to low affinity regulatory domain. Upon close inspection of the binding isotherm, there appears to be a clear distinction between Ca^{2+} binding to the 2 structural C domain sites in the protein with inflections occurring at a molar ratio of approximately 1 and 2.

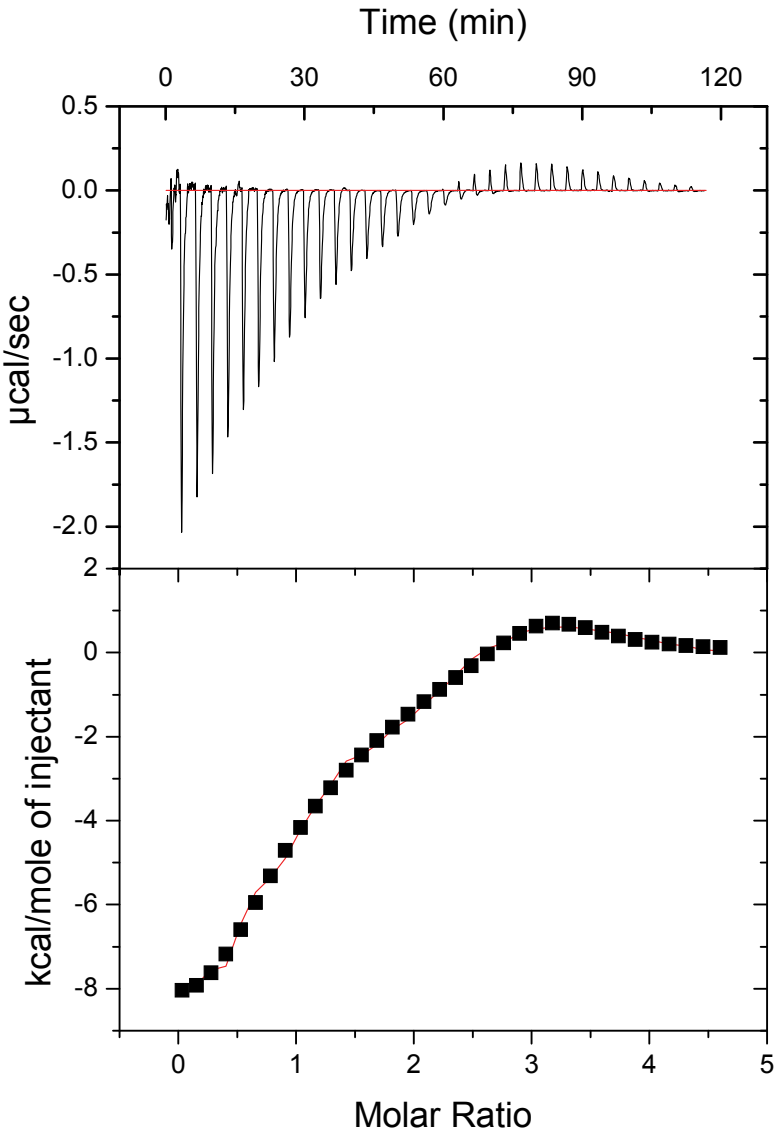

Figure 4.7. **A** titration of Ca^{2+} (1 mM) into apo HCTnC (44.6 µM). Data was fit using a sequential set of sites binding model. Experiments were conducted at room temperature (25^{o}C). All protein and metal solutions were in 10 mM MES and 50 mM KCl at pH=7.0 buffer conditions. Aliquots were delivered in 8 µL injections with a spacing of 250 s in between each injection. The stirring speed for the ITC was 307 rpm.

Table 4.4. Titration of Calcium into the apo form of HCTnC. This data set is fit to a sequential set of sites binding model.

Thermodynamic Parameters	**Average of 2 Data Sets**	**Reference [20, 45-47]**
K_1	1.03 (± 0.04) x 10^6	1 x 10^7
K_2	2.0 (± 0.4) x 10^5	1 x 10^7
K_3	3.8 (± 0.9) x 10^5	1 x 10^5
ΔG_1 (kcal/mol)	-8.2 (± 0.8)	
ΔG_2 (kcal/mol)	-7.2 (± 0.1)	
ΔG_3 (kcal/mol)	-7.6 (± 0.1)	
ΔH_1 (kcal/mol)	-8.6 (± 0.4)	
ΔH_2 (kcal/mol)	-5.5 (± 0.4)	
ΔH_3 (kcal/mol)	5 (± 1)	
$T\Delta S_1$ (kcal/mol)	-0.44 (± 0.36)	
$T\Delta S_2$ (kcal/mol)	1.7 (± 0.6)	
$T\Delta S_3$ (kcal/mol)	13 (± 1)	

As discussed in chapter 3, the binding constants in a "sequential set of sites" model are defined relative to the progress of saturation as seen in Eqs. 28-30.

$$K_1 = \frac{[MX]}{[M][X]} \qquad K_2 = \frac{[MX_2]}{[MX][X]} \qquad K_3 = \frac{[MX_3]}{[MX_2][X]}$$

Eqs. 28-30

The mechanism of metal binding to calmodulin, troponin, and other calcium-binding proteins has been widely investigated using fluorescence, ESI-MS techniques, and microcalorimetric studies [45-47, 50-51]. Data for calmodulin supports a cooperative binding mechanism that suggests a coupling between the four sites and two lobes of calmodulin [49]. A "sequential set of sites" model was therefore the best choice for fitting this data and the data is compiled in **Table 4.4**.

Addition of the first Ca^{2+} to HCTnC displays a binding constant, K_1, of 1.03 (± 0.04) x 10^6 which agrees quite closely to that found of BvCTnC (K_1 = 1.3 (± 0.1) x 10^6). These binding constant are 1 order of magnitude smaller than what is observed in the literature [21, 45-47]. The differences in binding constant values may stem from differences in buffers, buffer concentrations, ionic strength, and pH levels. Also, the values are closer to the Yamada paper when the temperature in increased [46]. In addition, the binding enthalpy ΔH_1 associated with the binding of the first ligand to the protein agrees quite nicely with that found for BvCTnC (-9.31 (± 0.04) kcal/mol) and differs by only a factor of 1.1. The $T\Delta S_1$ for this process was calculated to be -0.440 (± 0.362) kcal/mol. This differs from the value obtained for BvCTnC (-1.0 (± 0.1) kcal/mol) by a factor of two. The ΔG_1 was determined to be -8.2 (± 0.8) kcal/mol

which is very favorable. As a result, the binding of the first calcium ion to the protein is an enthalpically driven process.

The second calcium ion is shown to bind with a $K_2 = 2.0 (\pm 0.4) \times 10^5$ and $\Delta H_2 = -5.5 (\pm 0.4)$ kcal/mol. This is the first time that the binding of the second calcium ion has been distinctly observed by ITC for an EF handed protein. This contrasts data obtained for BvCTnC where binding of both ligands to the high affinity sites of the protein were indistinguishable. It is not clear as to whether this is due to differences in the amino acid sequences between BvCTnC and HCTnC or if the second binding was just not resolved in the BvCTnC titrations. Titrations involving BvCTnC were run at 10 μM concentrations, while titrations of HCTnC were run at much high concentrations (44 μM). ΔG_2 was found to be -7.2 (± 0.1) kcal/mol and energetically favorable. The entropy for this process was favorable as well with $T\Delta S_2 = 1.7 (\pm 0.6)$ kcal/mol. It is interesting to note that the binding constant obtained for calcium binding to the first site is an order of magnitude larger than binding to the second site. If both sites are identical, this would indicate a negative cooperativity between the two sites.

Binding of the third and final calcium to the protein is more comparable with that of the bovine titrations under the same conditions. The binding constant K_3 is $3.8 (\pm 0.9) \times 10^5$ and agrees closely with the literature value of the low affinity site (1×10^5) [21]. The overall ΔG_3 for this process is -7.6 (± 0.1) kcal/mol and energetically favorable as in the case of BvCTnC. ΔH_3 and ΔS_3 were found to be 5 (± 1) and 13 (± 1) kcal/mol respectively which differ from the BvCTnC values by a factor of 2 in each case. Again, this data reveals that binding of the third calcium is an entropically favored process.

4.5 Bepridil

A fundamental thermodynamic understanding of Bepridil's binding mechanism to cardiac troponin subunit C can reveal a multitude of answers regarding calcium sensitizers' viability as a drug treatment for familial hypertrophic cardiomyopathy. The following isothermal titration calorimetry experiments and discussions hopefully serve to answer some of these questions regarding Bepridil and calcium sensitizing drugs' mechanism of action.

Bepridil is known to make troponin more sensitive to the presence of calcium as a "calcium sensitizer." Bepridil is also acknowledged to only bind to troponin in the presence of calcium. As discussed in the previous chapter, Bepridil binds three equivalents to the C subunit of troponin in isolation [42]. When the entire complex of troponin is present, Bepridil has only been shown to bind one equivalent. Our study will only focus on the C subunit of troponin.

Possibly the most important experiments in terms of understanding the mechanism by which Bepridil binds to cardiac troponin subunit C are the titrations involving Bepridil with the human form of the protein. We were able to get successful titration data where one can observe the binding of the three equivalents of Bepridil to the calcium saturated form of the protein. This process was not easy. Bepridil is not very soluble in water and must first be diluted in ethanol before going into solution. pH is another issue associated with Bepridil. Bepridil needs to be at a relatively low pH in order for it to stay in solution and not precipitate out of the solution. Our threshold of pH allowed for us to be the closest to a neutral pH that we could be without the drug crashing out of solution. A pH of 5.7 was used in all Bepridil titrations. We also made sure that the pH of the protein was the same so as to only detect heats associated with the binding of the drug to the protein.

A) Bepridil Binding to HCTnC

Figure 4.8 displays a typical binding isotherm found when titrating Bepridil into HCTnC in the presence of 10 mM $CaCl_2$. The isotherm looks very different from those obtained in the calcium binding experiments. The titration produced solely exothermic peaks that reached heat of dilution at a molar ratio of 7. The titrations were not extended further. The isotherm does not display predominant features, but upon closer inspection it appears to have two phases. The first phase in the isotherm is characterized by a steep slope which tapers off at a molar ratio of 2. This phase is followed by a gentler slope that slowly reaches heat of dilution.

As mentioned previously, 3 Bepridil molecules bind to CTnC in the absence of the TnI and TnT subunits [42]. More specifically, x-ray crystal structures have revealed two Bepridil molecules bind to the C lobe of the protein whereas the third molecule binds to the N lobe of the protein [42]. It is not known what the order of the binding is or if there is cooperativity between the binding sites. Fitting the data to the simplest model available to us, the "one set of sites" model, did not result in a proper fit to the data. We chose the "two set of sites" model because there were only 2 discernable phases in the data retrieved. This does not necessarily mean that there are only 2 Bepridil molecules that bind, but it appears that there are only two phases of binding which may mean the binding of 2 Bepridil molecules shadow one another. The thermodynamic data is compiled in **Table 4.5**.

Binding of Bepridil molecules to HCTnC is an energetically favorable process in two phases as noted by the ΔG values in **Table 4.5**. Binding constants for the processes are on the order of 10^5 (1^{st} phase) and 10^4 (2^{nd} phase). Both binding constants reveal enthalpically driven processes with ΔH_1 and ΔH_2 values of -16.16 (± 4.34) kcal/mol and -27.17 (± 5.76) kcal/mol,

respectively. Entropy was disfavored in these two processes with TΔS values equal to -10.22 (± 4.32) and -20 (± 6.02) kcal/mol for each binding event.

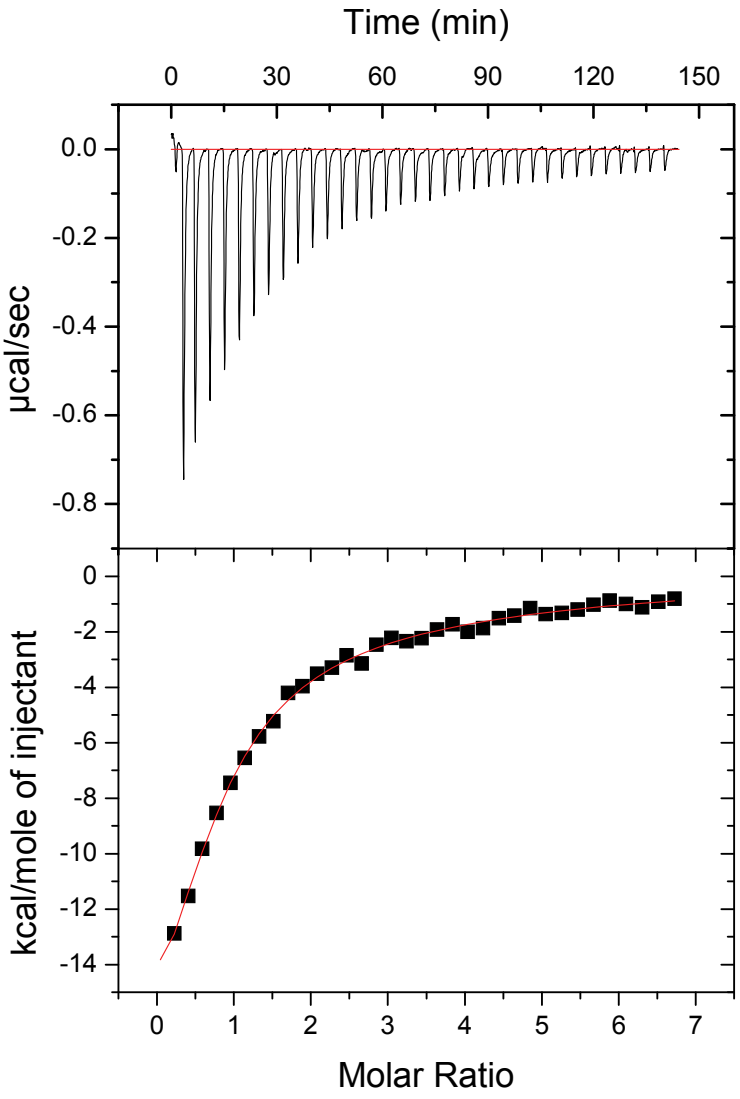

Figure 4.8. A titration of Bepridil (0.295 mM) into HCTnC (9 µM) containing $CaCl_2$ (10 mM). Bepridil stocks were dissolved in 5% EtOH. Experiments were conducted at room temperature (25^{o}C). All protein and metal solutions were in 10 mM MES and 50 mM KCl at pH=5.7 buffer conditions. All solutions were matched with identical amounts of EtOH. Aliquots were delivered in 8 µL injections with a spacing of 250 s in between each injection to ensure equilibration. The stirring speed for the ITC was 307 rpm.

Table 4.5. Thermodynamic Properties of Bepridil Titrated into HCTnC with Ca^{2+} Present.

Thermodynamic Parameters	**Average of 2 Data Sets**
n_1	1 (± 0)
n_2	0.62 (± 0.05)
K_1	2.23 (± 0) x 10^4
K_2	1.97 (± 0.85) x 10^5
β	4.39 (± 0.85) x 10^9
ΔG_1 (kcal/mol)	-5.92 (± 0)
ΔG_2 (kcal/mol)	-7.17 (± 0.27)
ΔH_1 (kcal/mol)	-16.16 (± 4.34)
ΔH_2 (kcal/mol)	-27.17 (± 5.76)
$T\Delta S_1$ (kcal/mol)	-10.22 (± 4.32)
$T\Delta S_2$ (kcal/mol)	-20.00 (± 6.02)

Based on our data, it is not possible to deduce a third binding event in the binding isotherm or in the raw data. There are only two phases of binding occurring and it is not possible to discern a third binding event in the data. Early NMR studies suggest very large changes in the protein upon binding up to 1 equivalent of Bepridil [40]. These changes become less pronounced upon binding additional equivalents. Furthermore, these changes occur in the spectral regions that correspond to the regulatory domain of the protein. According to the NMR structure, binding of Bepridil to the regulatory domain (N Lobe) results in a large conformational change [40]. This change opens the regulatory lobe and exposes a hydrophobic patch [40]. Based on this information, we hypothesize that the first set of thermodynamic parameters refers to the binding of a Bepridil molecule to the N domain region of the protein. To verify this, it would be worthwhile to study the truncated N domain form of the protein for comparison.

The sequential mechanism of Bepridil binding to a TnC protein is shown in scheme 1.

$$\text{Bep} + \text{TnC} \xrightarrow{K_1} \text{Bep-TnC}$$

$$\text{Bep-TnC} + \text{Bep} \xrightarrow{K_2} \text{Bep}_2\text{-TnC}$$

Scheme 1.

The overall binding reaction and binding constant, β, for 3 Bepridil molecules binding to TnC is represented by Equations 31 and 32 respectively.

$$2\,\text{Bep} + \text{TnC} \xrightarrow{\beta} \text{Bep}_2\text{-TnC}$$

Eq. 31

$$\beta = \frac{[Bep_2 - TnC]}{[Bep]^2[TnC]}$$

Eq. 32

The β value can be calculated according to the following expression.

$$K_1 \text{ x } K_2 = \beta$$

Eq. 33

The β value for this process was found to be 4.39 x 10^9. Early studies report an apparent binding constant of 1 x 10^5 for Bepridil binding to CTnC by fluorescent methods [52]. It is important to note that the conditions under which these experiments were run differed from ours and also did not account for competing reactions. It is also important to note that our value represents two Bepridil binding events to the protein and is not relevant physiologically.

4.6 Conclusions

A) Divalent Metal Binding Conclusions

I. Calcium Binding (BvCTnC)

- The K_1 for the "two set of sites" model and the K_1/K_2 for the "sequential set of sites" model is an order of magnitude less than what is reported in the literature, but closer to the Yamada paper value when done at a similar temperature and using similar techniques
- The K_2 for the "two set of sites" model and the K_3 for the "sequential set of sites" model agrees well with the literature.
- The binding of the two high affinity sites are enthalpically driven processes.
- The binding of the low affinity site is an entropically driven process.

II. Magnesium Binding (BvCTnC)

- The ITC experiments where magnesium is titrated into the apo form of the protein proved unsuccessful. This may be an indication that the heats associated with the binding events are beyond the threshold of the instrument.

- The experiments where Mg^{2+} is displaced by Ca^{2+} from the three binding sites were done at low concentrations of Mg^{2+}. Future studies may look to increase the concentration of Mg^{2+} to properly report thermodynamic properties associated with competition for the binding sites.

III. Calcium Binding (HCTnC)

- Unique because thermodynamic parameters were extracted for the binding events of each of the three calcium ions to the apo form of HCTnC.
- The 3rd site is an entropically driven process and sites 1 and 2 are enthalpically driven processes.
- It is interesting to note that $K_1 > K_2$ because it implies that binding of calcium is not cooperative and binding of the first calcium weakens the binding of the second calcium.

B) Bepridil Binding Conclusions

- Binding of Bepridil to HCTnC occurs in two phases.
- The two binding events appear to be enthalpically driven processes.
- One binding event binds with a higher affinity than the other.

C) Future Directions

The calcium and Bepridil ITC studies with bovine and human forms of the cardiac TnC protein have produced very interesting results. ITC has allowed us to directly observe and quantify, for the first time, the ΔH and ΔS of binding to this system. In particular, experiments revealed that calcium binding to the regulatory domain is an entropically driven process. This was not expected in light of the fact that a hydrophobic patch is exposed upon calcium binding to the N domain. This has forced us to think more deeply about the other changes in the protein that occur upon calcium binding to the regulatory domain of CTnC and has opened up a very important question. Are the thermodynamics of Ca^{2+} binding to the N domain affected by the presence of the C domain? In the absence of the C domain, will we see the same thermodynamic parameters for Ca^{2+} binding to the regulatory domain as observed in the full length protein?

We have recently obtained the construct for the truncated form of HCTnC which consists of the N domain region, residues 1-89. Future studies include over-expressing and purifying this protein according to already published procedures [53] and investigating its calcium and Bepridil binding properties.

Future studies also include investigating other possible "calcium sensitizing" drug molecules. Dr. Li and Dr. Huo are computationally designing and formulating new drugs that may fit as drugs to treat this disorder. Our first attempts at studying such molecules were unsuccessful. This was mainly due to solubility issues which need to be resolved.

References

1. Huxley, A.F., Niedergerke, R., Structural changes in muscle during contraction-Interference microscopy of living muscle fibres. *Nature* **173**: 973-976 (1954).

2. Huxley, H., Hanson, J., Changes in the cross-striations of muscle during contraction and stretch and their structural interpretation. *Nature* **172**: 530-532 (1953).

3. Retrieved from http://upload.wikimedia.org/wikipedia/commons/c/c0/Skeletal_muscle.jpg. Accessed 2010.

4. Lodish, H., Berk, A., Zipursky, S.L., Matsudaira, P., Baltimore, D., Darnell, J., **Molecular Cell Biology. 4th Ed**., New York, New York, W.H. Freeman and Company, (1999).

5. Retrieved from http://upload.wikimedia.org/wikipedia/commons/a/a4/Sarcomere.gif. Accessed 2010.

6. Oakley, C.E., Hambly, B.D., Curmi, P.M.G., Brown, L.J., Myosin binding protein C: Structural abnormalities in familial hypertrophic cardiomyopathy. *Cell Research* **14**: 95-110 (2004).

7. Ebashi, S., Endo, M., Ohtsuki, I., Control of muscle contraction. *Quarterly Reviews of Biophysics* **2(4)**: 351-384 (1969).

8. Retrieved from http://www.unmc.edu/physiology/Mann/mann14.html. Accessed 2008.

9. Retrieved from http://labs.ansci.uiuc.edu. Accessed 2008.

10. Gafurov, B., Fredricksen, S., Cai, A., Brenner, B., Chase, P.B., Chalovich, J.M., The Δ14 mutation of human cardiac troponin T enhances ATPase activity and alters cooperative binding of S1-ADP to regulated actin. *Biochemistry* **43**: 15276-15285 (2004).

11. Ebashi, S., Third component participating in superprecipitation of actomyosin. *Nature* **200**: 1010 (1963).

12. Gusev, N.B., Friedrich, P., Ca(2+)-induced conformational changes in the troponin complex detected by crosslinking. *Biochemica et. Biophysica Acta, Protein Structure* **626**: 106-116 (1980).

13. Takeda, S., Yamashita, A., Maeda, K., Maeda, Y., Structure of the core domain of human cardiac troponin in the Ca(2+)-saturated form. *Nature* **424**: 35-41 (2003).

14. Cowan, J.A. *Inorganic Biochemistry: an introduction*. Wiley-VCH, Inc. (1997).

15. Strynadka, N.C.J, James, M.N.G., Crystal structures of the helix-loop-helix calcium-binding proteins. *Annual Reviews of Biochemistry*. **58**: 951-998 (1989).

16. Kretsinger, R.H., Nockolds, C.E., Carp muscle calcium-binding protein. 2. Structure determination and general description. *Journal of Biological Chemistry*. **248**: 3313-3326 (1973).

17. Berg, J., Tymoczko, J., Stryer, L., **Biochemistry. 6th Ed.**, New York, New York, W.H. Freeman and Company, (2007).

18. Busch, E., Hohenester, E., Timpl, R., Paulsson, M., Calcium affinity, cooperativity, domain interactions of extracellular EF-hands present in BM-40. *Journal of Biological Chemistry*. **275**: 25508-25515 (2000).

19. Retreived from http://upload.wikimedia.org/wikipedia/commons/7/78/EFhandmotif.jpg. Accessed 2010.

20. Cheung, W.Y., **Calcium and Cell Function (Molecular Biology)**. Academic Press, (1982).

21. Rosenfeld, S.S., Taylor, E.W., Kinetic studies of calcium and magnesium binding to troponin C. *Journal of Biological Chemistry*. **260**: 242-251 (1985).

22. Li, M.X., Wang, X., Sykes, B.D., Structural based insights into the role of troponin in cardiac muscle pathophysiology. *Journal of Muscle Research and Cell Motility*. **25**: 559-579 (2004).

23. Potter, J.D., Gergely, J., The calcium and magnesium sites on troponin and their role in the regulation of myofibiliar adenosine triphosphate. *Journal of Biological Chemistry*. **250**: 4628-4633 (1975).

24. Labugger, R., Organ, L., Collier, C., Atar, D., Van Eyk, J.E., Extensive troponin I and T modification detected in serum from patients with acute myocardial infarction. *Circulation*. **102**: 1221-1226 (2000).

25. Gomes, A.V., Potter, J.D., Cellular and molecular aspects of familial hypertrophic cardiomyopathy caused by mutations in the cardiac troponin I gene. *Molecular and Cellular Biochemistry*. **263**: 99-114 (2004).

26. Ohtsuki, I., Molecular arrangement of troponin T in the thin filament. *Journal of Biochemistry*. **86**: 491-497 (1979).

27. Malnic, B., Farah, C.S., Reinach, F.C., Regulatory properties of the NH2 and COOH-terminal domains of troponin T. ATPase activation and binding to troponin I and troponin C. *Journal of Biological Chemistry*. **273**: 10594-10601 (1998).

28. Retrieved from http://www.microcal.com/technology/itc.asp. Accessed 2008.

29. A model adaptation from the Wilcox group at Dartmouth University. Received 2008.

30. ITC Data Analysis in Origin, Manual Version 7.0, January 2004, Accessed 2008.

31. Ward, W.H.J., Holdgate, G.A., Isothermal titration calorimetry in drug discovery. *Progress in Medicinal Chemistry*. **38**: 309-376 (2001).

32. Williams, D.H., O'Brien, D.P., Sandercock, A.M., Stephens, E., Order changes within receptor systems upon ligand binding: receptor tightening/oligomerisation and the interpretation of binding parameters. *Journal of Molecular Biology*. **340**: 373-383 (2004).

33. Lambert, F.L., Disorder – a cracked crutch for entropy discussions. *Journal of Chemical Education*. **79**: 187-192 (2002).

34. Cabani, S., Gianni, P., Mollica, V., Lepori, L., Group contributions to the thermodynamic properties of nonionic inorganic solutes in dilute aqueous solution. *Journal of Solution Chemistry*. **10**: 563-595 (1981).

35. Maron, B.J., Gardin, J.M., Flack, J.M., Gidding, S.S., Kurosaki, T.T., Bild, D.E., Prevalence of hypertrophic cardiomyopathy in a general population of young adults. Endocardiographic analysis of 4111 subjects in the CARDIA study. Coronary artery risk development in (young) adults. *Circulation*. **92**: 785-789 (1995).

36. Retrieved from http://www.medterms.com/script/main/art.asp?articlekey=13592. Accessed 2009.

37. Maron, B.J., Pelliccia, A., Spirito, P., Cardiac disease in young trained athletes. Insights into methods for distinguishing athlete's heart from structural heart disease, with particular emphasis on hypertrophic cardiomyopathy. *Circulation*. **91**: 1596-1601 (1995).

38. Watkins, H., Hypertrophic cardiomyopathy: from molecular and genetic mechanisms to clinical management. *European Heart Journal Supplements*. **3**: L43-L50 (2001).

39. Cirino, A.L, Ho, C., Familial hypertrophic cardiomyopathy overview. *Gene Reviews (Internet)*. Updated: May 26, 2009. Accessed 2009.

40. MacLachlan, L.K., Reid, D.G., Mitchell, R.C., Salter, C.J., Smith, S.J., Binding of calcium sensitizer, bepridil, to cardiac troponin C. A flourescence stopped-flow kinetic, circular dichroism, and proton nuclear magnetic resonance study. *Journal of Biological Chemistry*. **265**: 9764-9770 (1990).

41. Retrieved from http://www.rxlist.com/vascor-drug.html. Accessed 2009.

42. Li, Y., Love, M.L., Putkey, J.A., Cohen, C., Bepridil opens the regulatory N-lobe of cardiac troponin C. *Proceedings from the National Academy of Sciences of the United States of America*. **97**: 5140-5145 (2000).

43. Retrieved from http://www.sigmaaldrich.com/life-science/metabolomics/enzyme-explorer/learning-center/protease-inhibitors.html. Accessed 2009.

44. Cheung, H.C., Wang, C.K., Garland, F., Fluorescence energy transfer studies of skeletal troponin C proximity between methionine-25 and cysteine-98. *Biochemistry*. **21**: 5135-5142 (1982).

45. Yamada, K., The enthalpy titration of troponin C with calcium. *Biochimica et Biophysica Acta*. **535**: 342-347 (1978).

46. Yamada, K., Kometani, K., Enthalpy, entropy, and heat capacity changes induced by binding of calcium ions to cardiac troponin C. *Biochemical and Biophysical Research Communications*. **114**: 162-167 (1983).

47. Yamada, K., Thermodynamic analyses of calcium binding to troponin C, calmodulin and parvalbumins by using microcalorimetry. *Molecular and Cellular Biochemistry*. **190**: 39-45 (1999).

48. EDTA-$CaCl_2$ Test Kit Instructions for VP-ITC. Accessed 2009.

49. Gilli, R., Lafitte, D. Lopez, C., Kilhoffer, M.-C., Makarov, A., Briand, C., Haeich, J., Thermodynamic analysis of calcium and magnesium binding to calmodulin. *Biochemistry*. **37**: 5450-5456 (1998).

50. Shirran, S.L., Barran, P.E., The use of ESI-MS to probe the binding of divalent cations to calmodulin. *Journal of the American Society for Mass Spectrometry*. **20**: 1159-1171 (2009).

51. LaPorte, D.C., Keller, C.H., Olwin, B.B., Storm, D.R., Preparation of fluorescent-labeled derivative of calmodulin which retains its affinity for calmodulin binding proteins. *Biochemistry*. **20**: 3965-3972 (1981).

52. Solaro, R.J., Bousquet, P., Johnson, J.D., Stimulation of cardiac myofilament force, ATPase activity and troponin C Ca++ binding by bepridil. *Journal of Pharmacology and Experimental Therapeutics*. **238**: 502-507 (1986).

53. Kilhoffer, M.-C., Kubina, M., Travers, F., Haiech, J., Use of engineered proteins with internal tryptophan reporter groups and perturbation techniques to probe the mechanism of ligand-protein interactions; investigation of the mechanism of calcium binding to calmodulin. *Biochemistry*. **31**: 8098-8106 (1992).

Appendix A

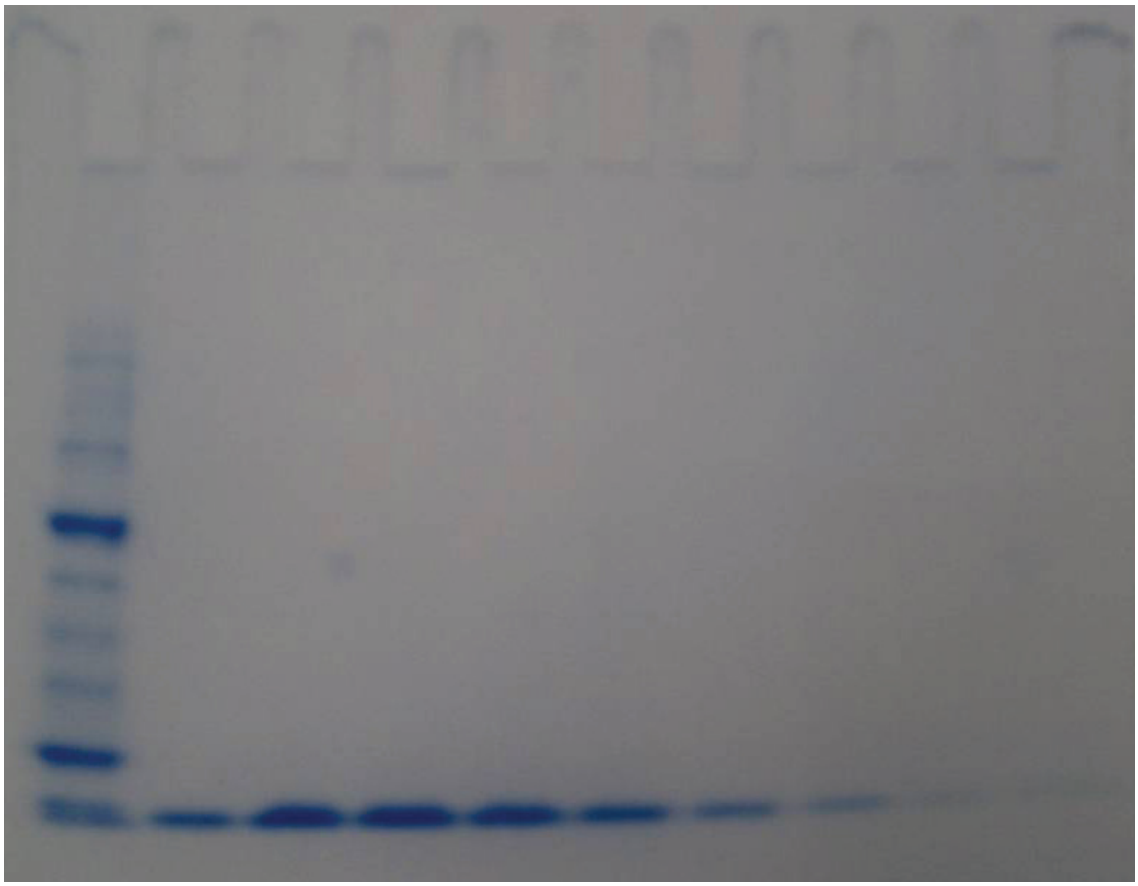

A) Supplemental gel to compare to **Figure 4.1.** Similar conditions to the gel reported previously in the thesis.

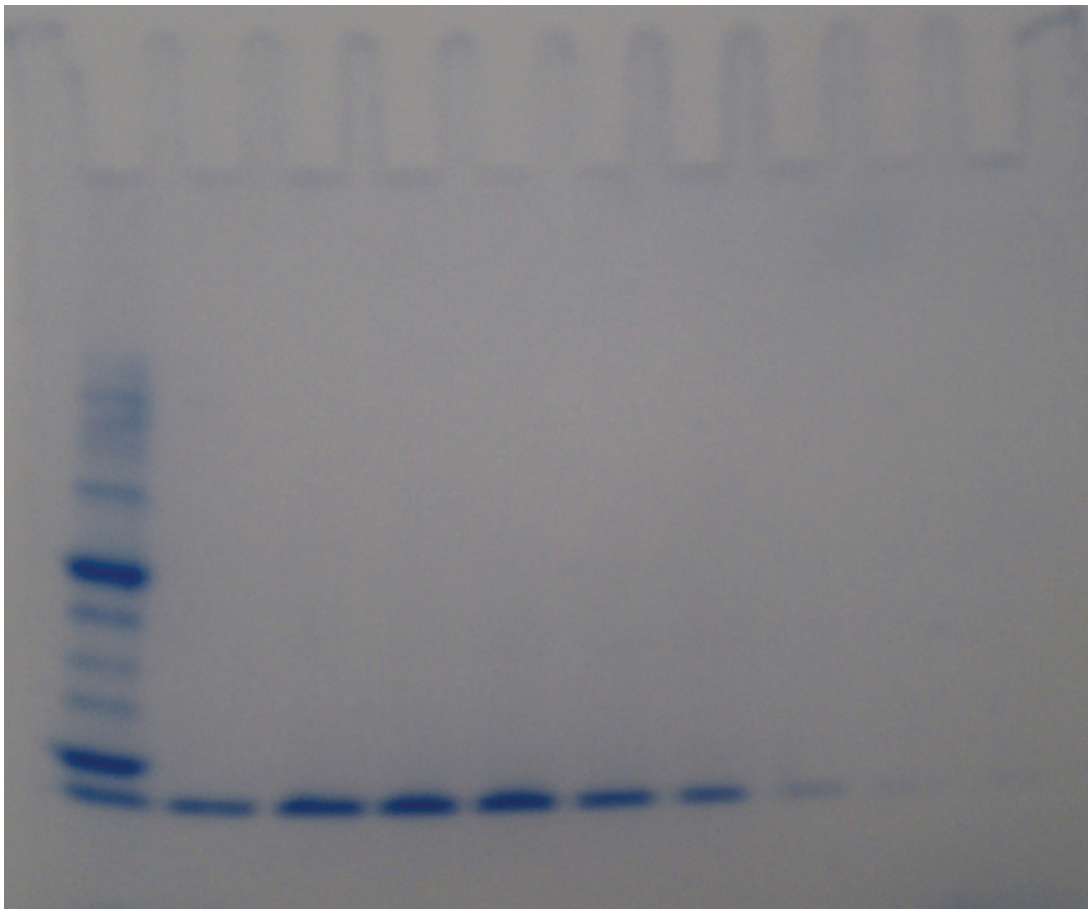

B) Supplemental to compare to **Figure 4.1.** Similar conditions to the gel reported previously in the thesis.

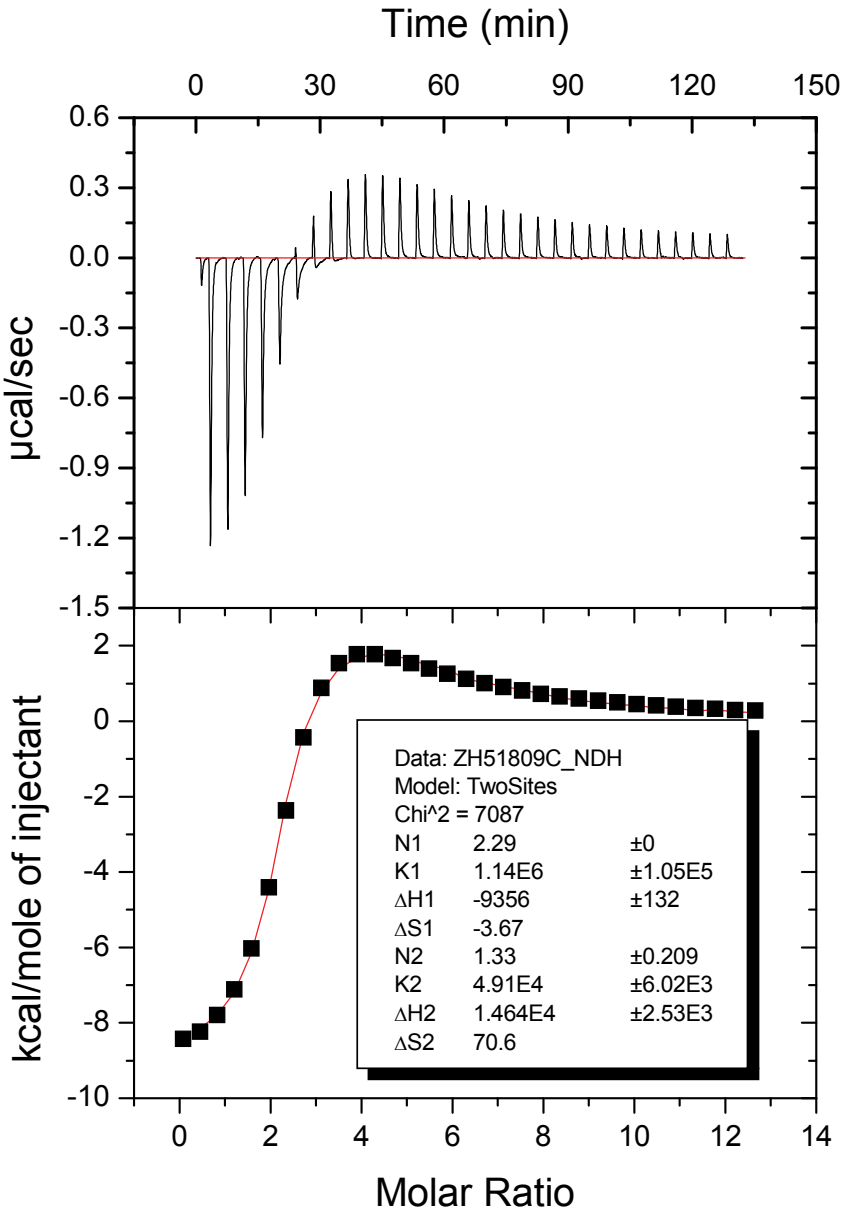

C) Supplemental data to compare to **Figure 4.3.** A titration of Ca^{2+} (0.6 mM) into apo BvCTnC (10 µM). Experiments were conducted at room temperature (25°C). All protein and metal solutions were in 10 mM MES and 50 mM KCl at pH=7.0 buffer conditions. Aliquots were delivered in 8 µL injections with a spacing of 250 s in between each injection. The stirring speed for the ITC was 307 rpm. This data set was fit to a "two set of sites" binding model.

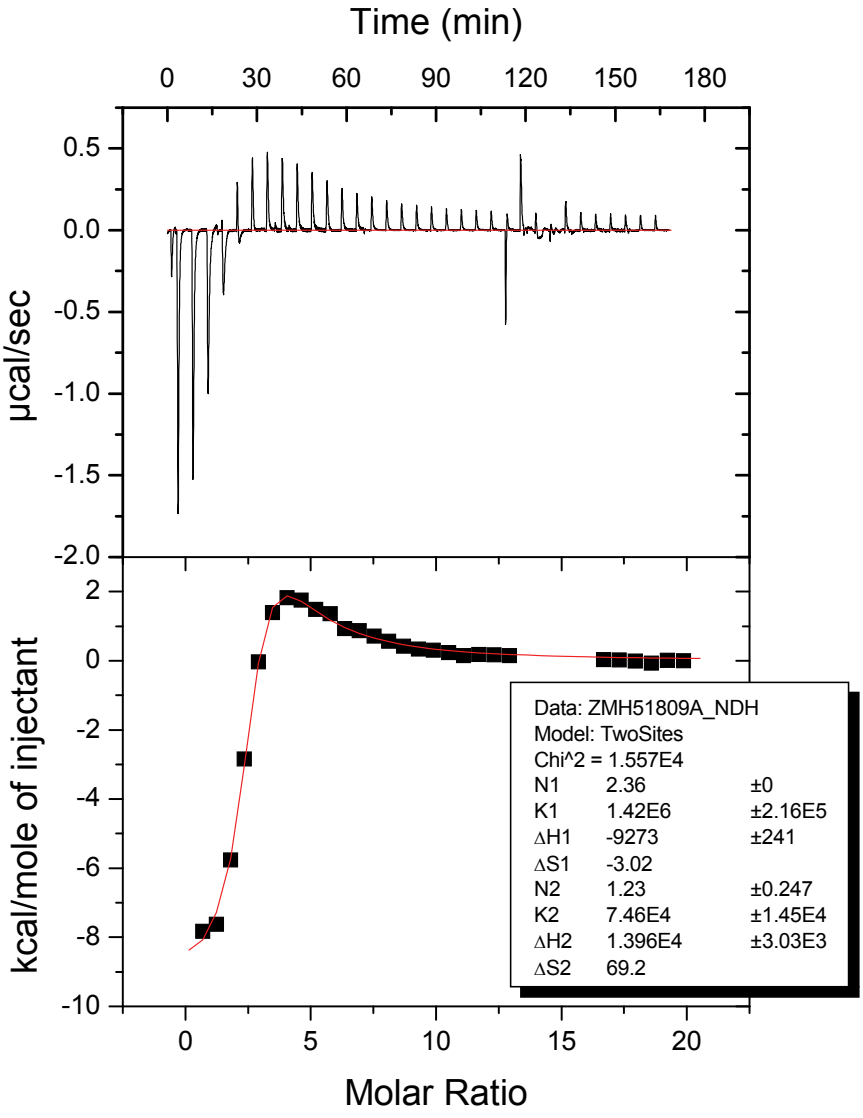

D) Supplemental data to compare to **Figure 4.3**. A titration of Ca^{2+} (1 mM) into apo BvCTnC (10 µM). Experiments were conducted at room temperature (25°C). All protein and metal solutions were in 10 mM MES and 50 mM KCl at pH=7.0 buffer conditions. Aliquots were delivered in 8 µL injections with a spacing of 250 s in between each injection. The stirring speed for the ITC was 307 rpm. This data set was fit to a "two set of sites" binding model.

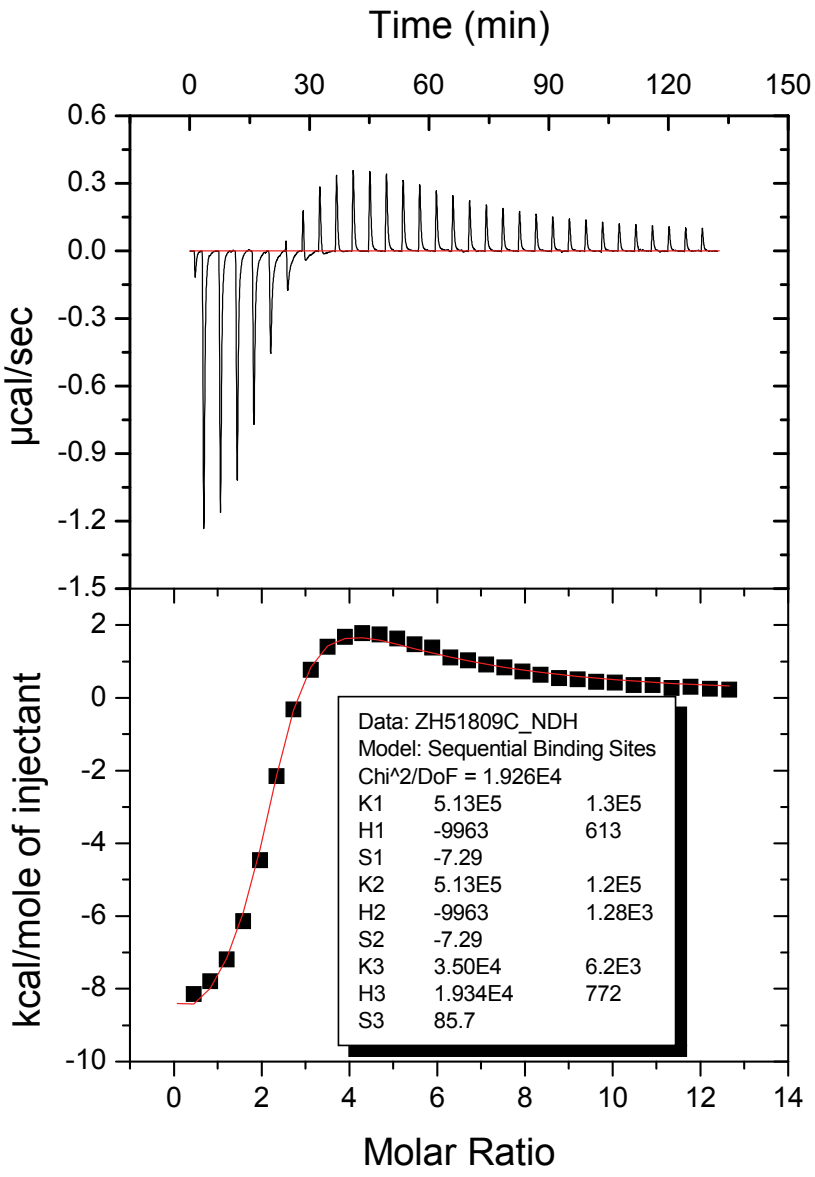

E) Supplemental data to compare to **Figure 4.4**. A titration of Ca^{2+} (0.6 mM) into apo BvCTnC (10 µM). Experiments were conducted at room temperature (25°C). All protein and metal solutions were in 10 mM MES and 50 mM KCl at pH=7.0 buffer conditions. Aliquots were delivered in 8 µL injections with a spacing of 250 s in between each injection. The stirring speed for the ITC was 307 rpm. This data set was fit to a "sequential set of sites" binding model.

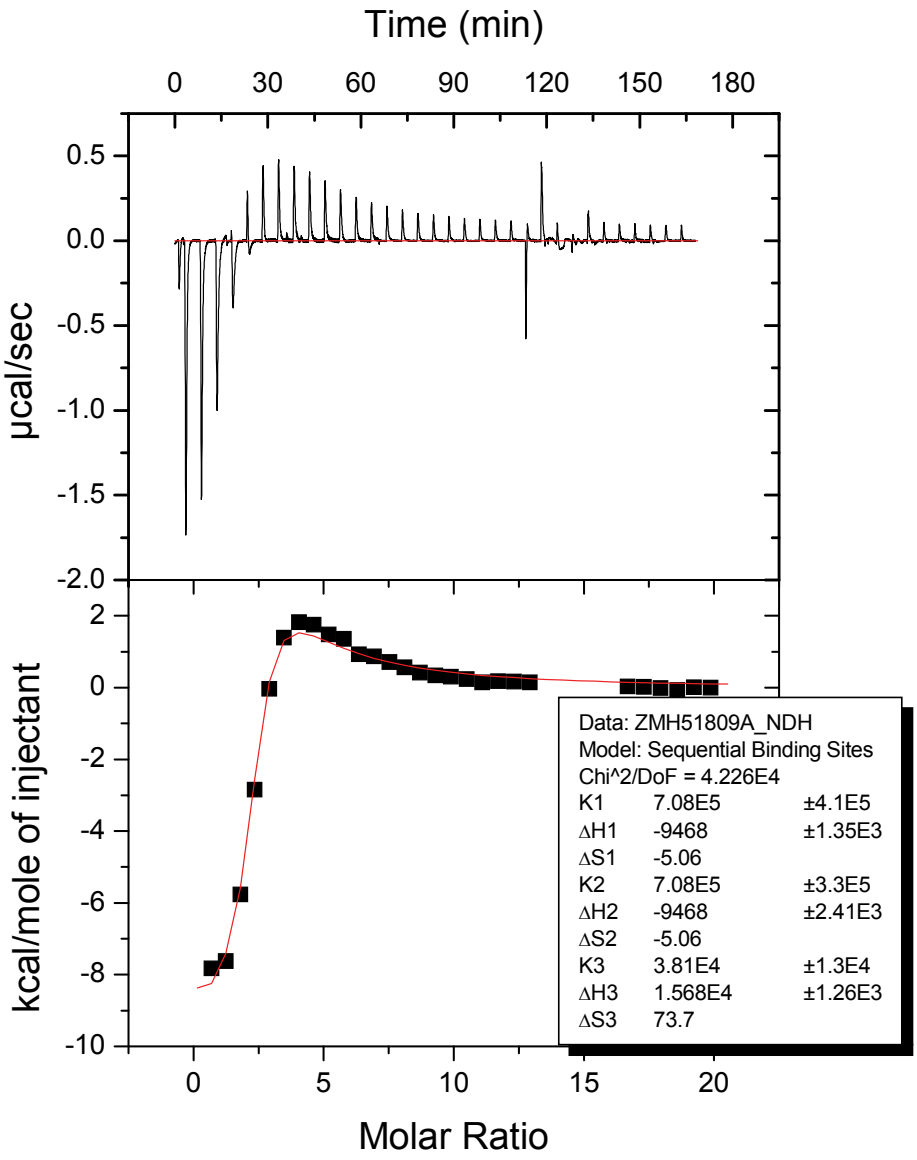

F) Supplemental data to compare to **Figure 4.4**. A titration of Ca^{2+} (1 mM) into apo BvCTnC (10 µM). Experiments were conducted at room temperature (25°C). All protein and metal solutions were in 10 mM MES and 50 mM KCl at pH=7.0 buffer conditions. Aliquots were delivered in 8 µL injections with a spacing of 250 s in between each injection. The stirring speed for the ITC was 307 rpm. This data set was fit to a "sequential set of sites" binding model.

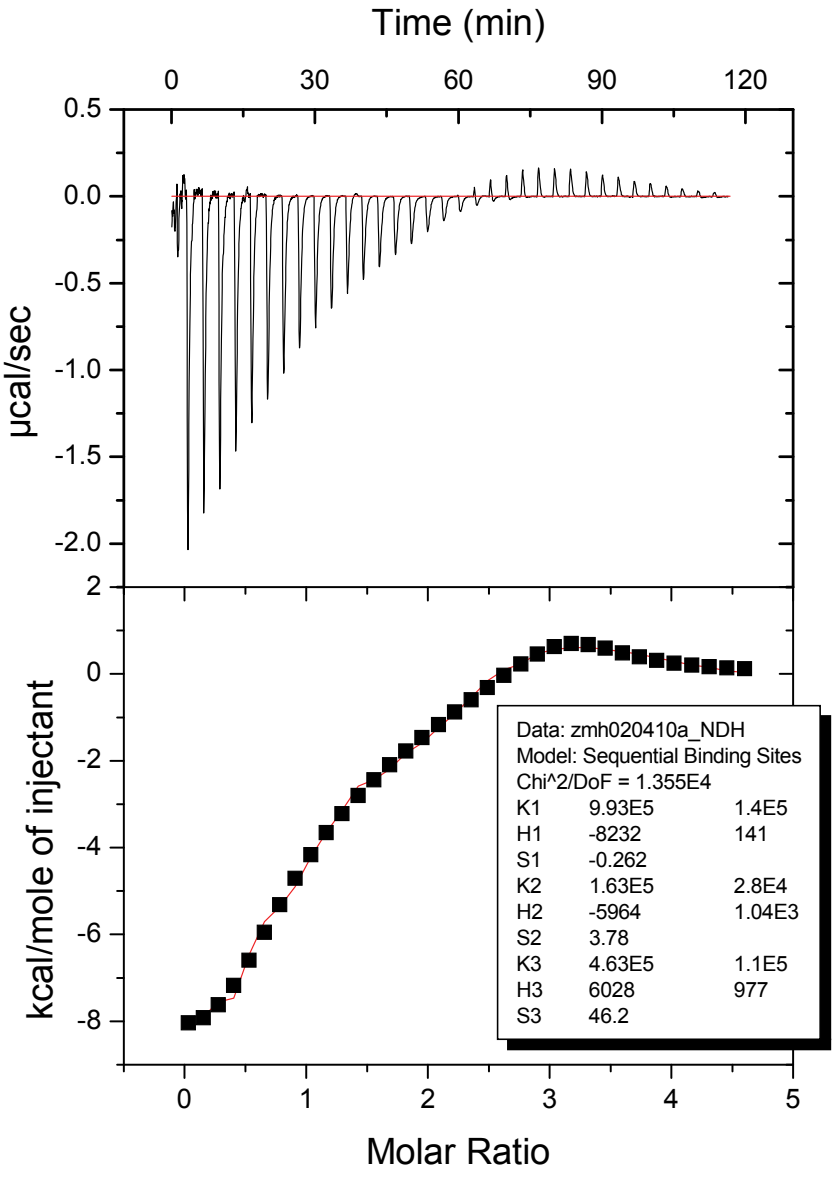

G) Supplemental data to compare to **Figure 4.7.** **A** titration of Ca^{2+} (1 mM) into apo HCTnC (44.6 µM). Data was fit using a sequential set of sites binding model. Experiments were conducted at room temperature (25^{o}C). All protein and metal solutions were in 10 mM MES and 50 mM KCl at pH=7.0 buffer conditions. Aliquots were delivered in 8 µL injections with a spacing of 250 s in between each injection. The stirring speed for the ITC was 307 rpm.

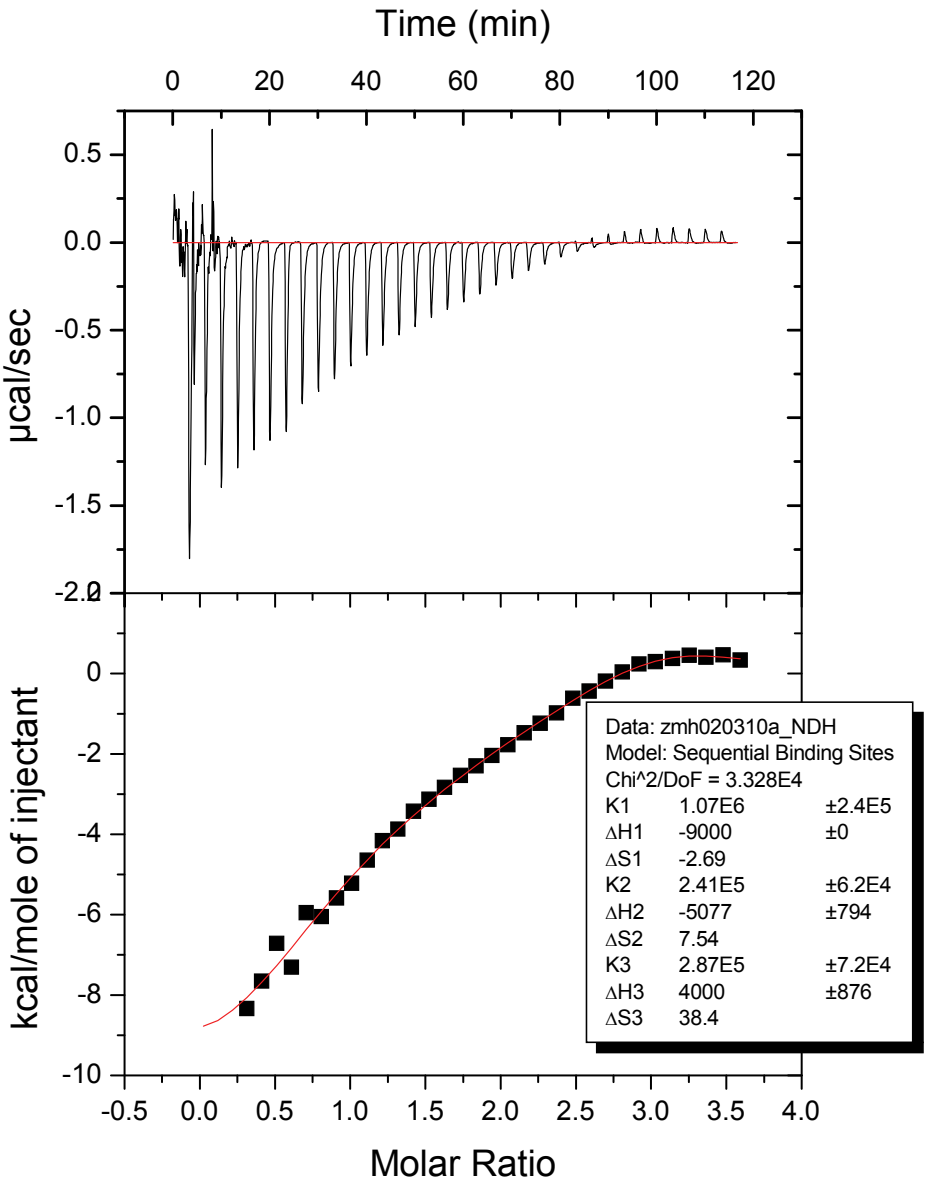

H) Supplemental data to compare to **Figure 4.7.** **A** titration of Ca^{2+} (0.7 mM) into apo HCTnC (44.6 µM). Data was fit using a sequential set of sites binding model. Experiments were conducted at room temperature (25°C). All protein and metal solutions were in 10 mM MES and 50 mM KCl at pH=7.0 buffer conditions. Aliquots were delivered in 8 µL injections with a spacing of 250 s in between each injection. The stirring speed for the ITC was 307 rpm.

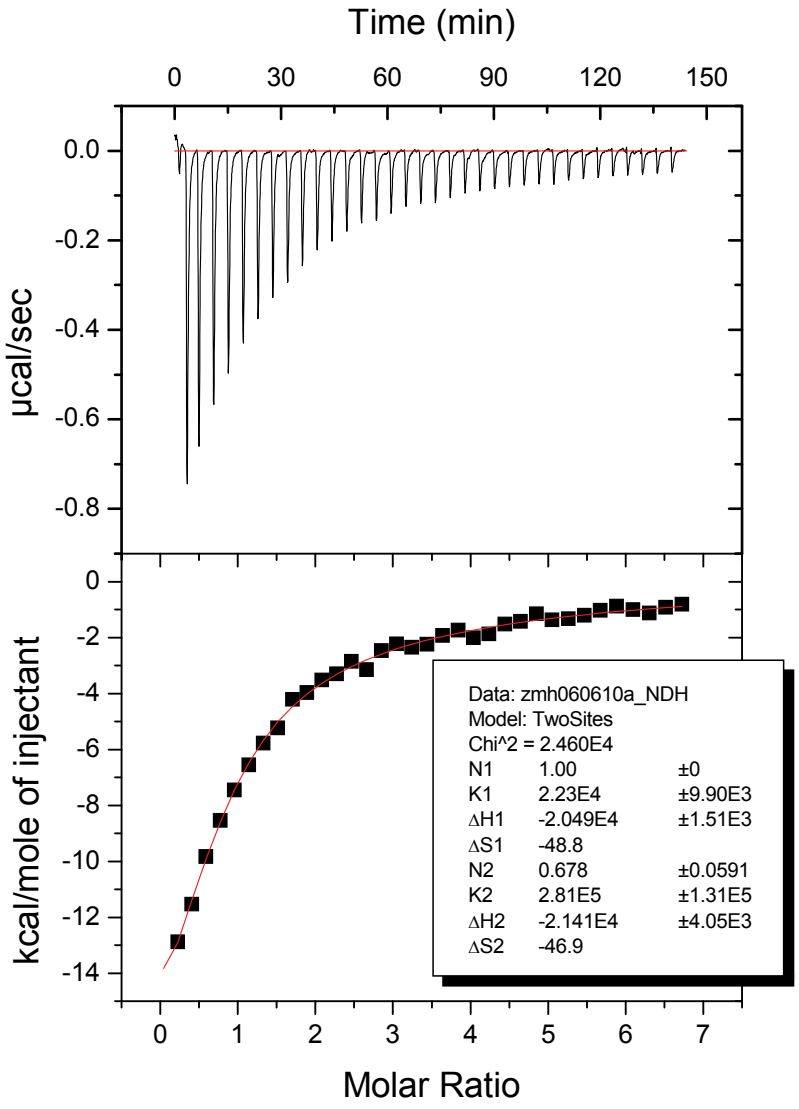

I) Supplemental data to compare to **Figure 4.8.** A titration of Bepridil (0.295 mM) into HCTnC (9 µM) containing $CaCl_2$ (10 mM). Bepridil stocks were dissolved in 5% EtOH. Experiments were conducted at room temperature (25°C). All protein and metal solutions were in 10 mM MES and 50 mM KCl at pH=5.7 buffer conditions. All solutions were matched with identical amounts of EtOH. Aliquots were delivered in 8 µL injections with a spacing of 250 s in between each injection to ensure equilibration. The stirring speed for the ITC was 307 rpm.

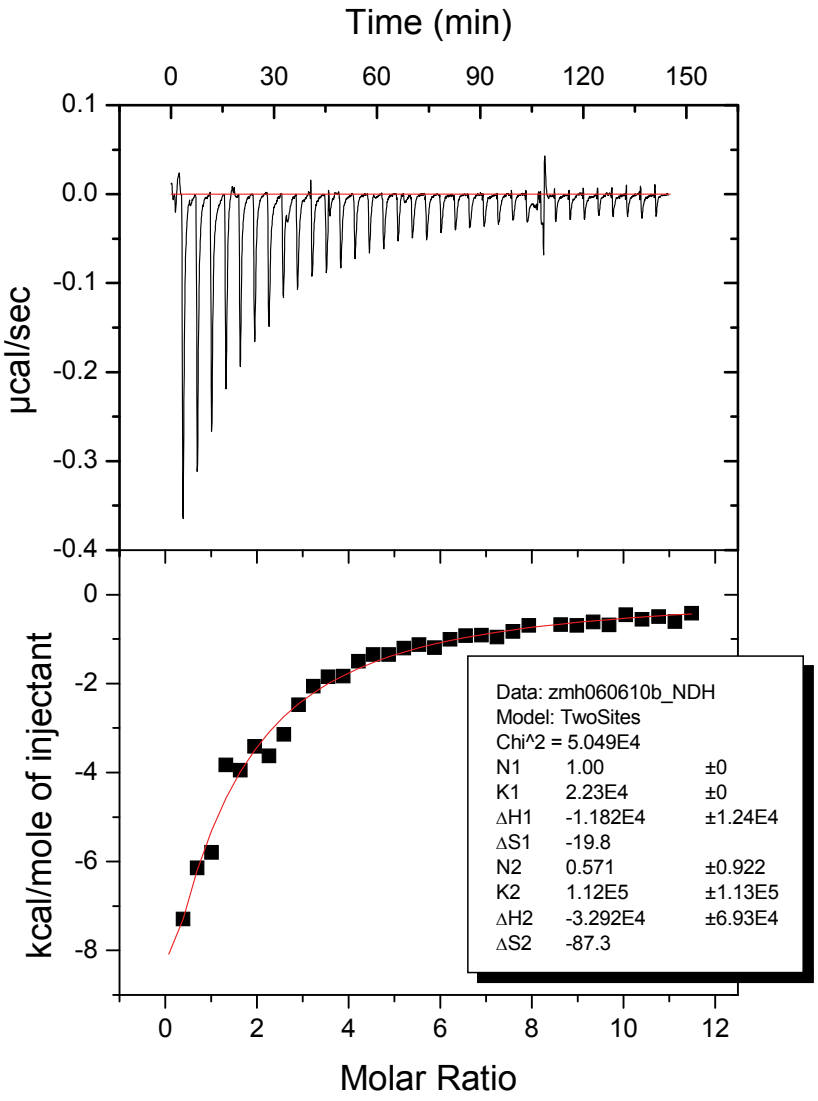

J) Supplemental data to compare to **Figure 4.8.** A titration of Bepridil (0.295 mM) into HCTnC (9 µM) containing $CaCl_2$ (10 mM). Bepridil stocks were dissolved in 5% EtOH. Experiments were conducted at room temperature (25°C). All protein and metal solutions were in 10 mM MES and 50 mM KCl at pH=5.7 buffer conditions. All solutions were matched with identical amounts of EtOH. Aliquots were delivered in 8 µL injections with a spacing of 250 s in between each injection to ensure equilibration. The stirring speed for the ITC was 307 rpm.